EVALUATION OF THE DURABILITY PROPERTIES OF GEOPOLYMER MORTAR SYNTHESIZED FROM TERNARY BLEND OF RICE HUSK ASH, CASSAVA PEEL ASH AND METAKAOLIN

BY

DAUDA, Ahmed Ayodeji

MTech/SET/2018/8181

DEPARTMENT OF BUILDING

FEDERAL UNIVERSITY OF TECHNOLOGY

MINNA

APRIL, 2023

ABSTRACT

The production of Geopolymer Mortar using Cassava Peel Ash (CPA), Metakaolin (MK) and Rice Husk Ash (RHA) as ternary blended Supplementary Cementitious Materials (SCM) has been proven recently to be an alternative way of reusing the agricultural and industrial waste materials with merits to dwindle the enormous amount of agricultural waste ash as well as the contribution in carbon footprint annually. Hence, studies also proved that the aggressive chemical curing media is still required for conventional geopolymer product in comparism with the ambient temperature media. The study therefore examined the durability properties of ternary blended Geopolymer Mortar (GPM) using Sodium Silicate (Na_2Si_3) and Sodium Hydroxide (NAOH) solution with 9M constant concentration as alkaline activators under both the aggressive and ambient-temperature curing media. The mass ratio of Sodium Silicate to Sodium Hydroxide (NS:NH) and as well as the binder to fine aggregate were fixed to 2.5 and 0.8 respectively. A series of fresh properties tests such as the setting time and the flow test were carried out and the durability of the ternary blended geopolymer mortar was examined through water absorption test, acid resistance test and sulphate resistance test using 50 mm cubes after 28, 56 and 90 days of curing. The results revealed that the setting time prolonged as the replacement levels of RHA-MK increased at a decrease in replacement levels of CPA. The results also showed that the mortar cured in sulphate solution as well as the sulphuric acid showed white precipitate on the Portland Cement Mortar (PCM) as the reference specimen with rounded edges and the GPM incorporated SCMs and activators (C90M7R3, C70M20R10, C50M33R17, C30M47R23 and C10M60R30) showed a little dark colour at all ages. The GPM was discovered to be more resistance to water absorption as compared to PCM while it was observed that the absorption increases as the hydration periods increases. Furthermore, both the PCM and GPM samples studied suffered mass and strength losses in both the acid and sulphate solution and the loss increased at an increase in the hydration periods, while the loss as caused by sulphuric acid is more pronounced. The losses were observed to be higher in PCM as compared to the GPMs while the mix incorporated 50% CPA, 33% MK and 17% RHA (C50M33R17) was observed to be better compared to other mixes in durability behaviour and the study therefore recommends C50M33R17 for good durability performance.

TABLE OF CONTENTS

LIST OF TABLES

LIST OF FIGURES

LIST OF PLATES

LIST OF ABBREVIATIONS

OPC	Ordinary Portland Cement
IEA	International Energy Agency
RHA	Rice Husk Ash
CPA	Cassava Peel Ash
MK	Metakaolin
SCSMS	Supplementary Cementitious Materials
BS	British Standard
(ASTM)	American Society for Testing and Materials
(PSD)	Particle Size Distribution
SLF	Strength Loss Factor
NAOH	Sodium Hydroxide
AAM	Alkali Activated Mortar

CHAPTER ONE

1.0 INTRODUCTION

1.1 Background to the Study

Over the years, Ordinary Portland Cement (OPC) has been widely employed as concrete binder and various building substances worldwide. It is known that, large scale manufacturing of OPC causes serious pollution in the environment in terms of considerable amount of greenhouse gases emission (Duxson *et al.,* 2007; Rashad *et al*., 2013). The OPC production alone is accountable for nearly 6 to 7% of total CO_2 emissions as estimated by International Energy Agency (IEA) (Palomo *et al.,* 2011). In fact, among all the greenhouse gases approximately 65% of the global warming is ascribed to the CO_2 emission. It was predicted that the mean temperature of the globe could rise by approximately 1.4–5.8°C over the next 100 years (Rehan & Nehdi, 2005). Globally, in the present backdrop of CO_2 emissions mediated climate change, the sea level is expected to rise and the frequent occurrence of natural disasters will cause huge economic loss (Stern, 2007). On top, the emitted greenhouse gases such as CO_2, SO_3 and NOx from the cement manufacturing industries can cause acid rain and damage the soil fertility (Zhang *et al*., 2011). Generally, the industrial consumption of raw materials is around 1.5 tonnes per each tonne of OPC production (Rashad, 2013a). To surmount such problems, scientists, engineers and industrial personnel have been continuously dedicating many efforts to develop novel construction materials to achieve alternate binders (Rashad, 2013b).

The term ‘‘geopolymers’’ was coined by Joseph Davidovits in 1972 (Komnitsas & Zaharaki, 2007) to describe the zeolite like polymers. Geopolymers that are being commonly synthesized by activating slag, Fly Ash (FA), calcined clay and other

aluminosilicate materials using alkali have been realized as promising alternative binders. Geopolymers are the alumino-silicate polymers which consist of three-dimensional amorphous structures formed due to the geopolymerization of alumino-silicate monomers in alkaline solution (Rowles & O'connor, 2003). In the past, intensive studies have been carried out on calcined clays (metakaolin) or industrial wastes such as fly ash palm oil fuel ash and slag (Chang, 2003; Kong *et al*., 2007; Temuujin *et al*., 2010). Yet, the complex process so called geopolymerization is not fully understood (Yao *et al*., 2009). Davidovits proposed a reaction pathway involving the polycondensation of orthosialiate ions (hypothetical monomer) (Provis *et al*., 2005). The mechanism of geopolymerization process (Dimas *et al*., 2009) is based on three steps: (i) dissolution in alkaline solution, (ii) reorganization and diffusion of dissolved ions with the formation of small coagulated structures and (iii) polycondensation of soluble species to form hydrated products. In recent years the name of alkali-activated has been used to replace the geopolymer name for a matrix using calcium in geopolymerization process.

Compared to OPC, alkali activated mortars are well-known for their excellent properties such as high compressive strength (Burciaga-Díaz *et al*., 2013; Zhang *et al*., 2010a), low shrinkage (Chi *et al*., 2012; Zhang *et al*., 2010a), acid resistance (Palomo *et al*., 1999), fire resistance, devoid of toxic fumes emission (Duxson *et al*., 2007), low thermal conductivity (Zhang *et al*., 2010a), excellent heavy metal immobilization, high temperature stability (Yao *et al*., 2009), low manufacturing energy consumption for construction purposes and several engineering applications (Zhang *et al*., 2010a). Owing to these distinctive features, Geopolymers are potentially being used in construction engineering, fire proof, biomaterials and waste treatment (Davidovits, 2002; Yao *et al*., 2009). New applications

Commented [D1]:

Commented [D2]:

Commented [D3]:

including the use of Geopolymer as concrete repair material is under in-depth exploration. In recent times, use of the alkali activated mortar as surface concrete repair materials has generated renewed research interests (Balaguru, 1998; Zhang *et al*., 2012; Zhang *et al*., 2010b). In the exploitation of the alkali activated mortar as repair material, the bond strength between the substrate concrete and the repair material (Geissert *et al*., 1999b; Momayez *et al*., 2005) plays a decisive role.

1.2 Statement of the Research Problem

Mortars and concretes made with Portland cement deteriorate in aggressive environment of sewers, mining, mineral processing, acid rain or acid ground-water (Harrison, 1987; Bakharev *et al*., 2003; Allahverdi & Skvara, 2005; Bakharev, 2005). Most of the commercial repair materials owing to their low durability and sustainability perform poorly under aggressive chemical and adverse weather environmental conditions. Although few epoxy repair materials display good performance. Geopolymer prepared from the waste materials with high content of aluminium-silicate and alkaline activator solution has emerged as a leading repair material. Geopolymeric binders are preferred because they generate 70-80% lesser CO_2 with remarkably reduced greenhouse gas emissions than Portland cement. However, new binders are prerequisite for enhanced durability performance, better sustainability and environmental friendliness.

Consequently, the present study intends to develop an environmental friendly geopolymer mortar with broad arrays of applications in the construction industry and exhibiting a durability characteristics by introducing three pozzolanic materials in enhancing the durability characteristics of the geopolymer mortar.

Commented [D4]:

Commented [D5]:

Commented [D6]:

Commented [D7]:

Commented [D8R7]:

Commented [D9]:

1.3 Aim and Objectives of the Research

The aim of this study is to evaluate the durability properties of geopolymer mortar synthesized from ternary blend of SHA, CPA and MK with a view to producing a zero cement mortar with low carbon foot print and enhanced durability.

The specific objectives are to:

i. Study the physical and chemical properties of RHA, CPA and MK constituents to develop a mixture proportion of ternary synthesized geopolymer mortars with enhanced durability.

ii. Determine the fresh properties of ternary blend geopolymer mortar.

iii. Evaluate the durability performance of the ternary blend geopolymer mortar.

1.4 Scope of Study

This research is experimental in nature and was mainly focused on the feasibility of achieving a new geopolymer mortars with enhanced durability. This new ternary blend geopolymer mortars was achieved by combining RHA, CPA and MK with appropriate proportions. The effects of various replacement of the supplementary cementitious materials (SCMs) blends on the durability properties of the synthesized geopolymer mortars was examined and various durability tests were performed to characterize the prepared geopolymer mortars. Materials characterizations was performed in terms of physical properties, chemical properties and mineralogical compositions.

To obtain the optimum ternary blend, tests on the properties of various ternary blended mixes were carried out with varying replacement levels, the minimum content of RHA (kept up to 25% by weight) and alkaline solution binder ratio ranged from 0.5 to 0.8.

Commented [D10]:

Commented [D11]:

Commented [D12]:

Commented [D13]:

Molarity of sodium hydroxide and the ratio of sodium silicate to sodium hydroxide are kept constant of 9 M and 2.5 respectively. The properties considered were mortar flow as well as acid and sulphate properties after curing in the solutions for 28, 56 and 90 days. The achieved optimum multi blend is further used for detail investigations on durability and microstructure properties.

The durability was assessed in terms of resistance of magnesium sulphate, sulphuric acid attack and water absorption resistance. The series of tests conducted were based on the procedures of British Standards (BS) and American Society for Testing and Materials (ASTM). International Union of Laboratories and Experts in Construction Materials, Systems and Structures is adopted in reviewing the literature. As these methods are being well established has enabled a comparison with related studies with information on their precision known.

1.5 Significance for the Study

This research intends to generate new data on the use of ternary blend geopolymer mortars by means of systematic methods of sample preparation from waste materials economically, appropriate and careful materials characterizations, and subsequent data analyses useful for the development of standard specifications for ternary blend geopolymer mortars system for diversified practical applications. This generated knowledge is expected to contribute to the development of environmental friendly and inexpensive geopolymer material for wide range of applications in the construction industry. This would be greatly beneficial for sustainable development of Nigeria, where wastes disposal problems towards the land filling can be avoided and minimized. The outcome of the study is believed to provide the basis for further researches and better understanding of the behaviour of a ternary blend

geopolymer mortar obtainable from the waste material in an economical and environmental affable manner.

CHAPTER TWO

2.0 LITERATURE REVIEW

2.1 Geopolymer

Geopolymers are a new class of binders that are manufactured through the reaction of three-dimensional alumino-silicate polymer materials in a concentrated alkaline solution (Hardjito, 2011**)**. These materials are amorphous to semi-crystalline in nature, with a crystal phase similar to zeolite structure. As earlier reported by Davidovits (1994), these classes of material possess numerous advantages ranging from high durability, and most importantly no danger with regards to alkali-aggregate reaction. Hitherto, research on geopolymers involves different manufacturing processes and the effect of synthesizing parameters on physical and mechanical properties (Thokchom *et al*., 2009). However, limited studies had been reported with regards to the durability of these classes of materials. Different natural materials such as thermally treated kaolin clay, metallurgical waste volcanic ash and byproducts (blast furnace slag, fly ash, cassava peel ash) have been utilized for the preparation of geopolymer material (Ogundiran & Kumar, 2015). But previous studies affirmed that sources, synthesis conditions, and intended uses of materials determine the characteristics of geopolymers. Owning to this feed, enhancing the properties of geopolymers materials is highly required to meet up the desired standard.

Commented [D14]:

2.2 Constituents of Geopolymer Material

The prominent components of geopolymer mortar are the source material and alkaline activator. The source materials which are the basic requirement for the

geopolymerization process to take place normally consist of a polymeric silicon-oxygen-aluminum framework with silicon and aluminum tetrahedral linked together in three-dimensional structures. Rangan (2014) highlighted that there are preferences regarding the source material used in the preparation of geopolymer. For instance, source materials that are highly rich in calcium content interfere with the microstructure of geopolymer mortar which could invariably compromise some benefits offered by geopolymer mortar. Whereas, those with low calcium content are preferred against those with the high calcium content.

2.3 Factors Affecting Geopolymer Strength Development

The properties and performance of geopolymer including strength and microstructure development, durability and workability of fresh geopolymer are significantly influenced by composition of blended binder, chemical composite of binder, alkali activator, water content and curing condition. The concentration and dosage of alkali activator affect the rate of geopolymerization and determine the final strength of hardened geopolymer. Besides, the molarity of activator solution would affect by the water content as well. Hydroxyl ions (water) in activator solution contribute to liberation of Si and Al from the geopolymer binder (Williamson & Juenger, 2016). However, excess in water content would dilute the concentration of activator.

2.3.1 Effect of alkali activator in strength development

Commented [D15]:

Commented [D16]:

Commented [D17]:

Alkali activator is added into geopolymer to improve the pH value of geopolymer mix with the primary purpose to enhance the dissolution of geopolymer binder. Therefore, the concentration and content of activator would vastly affect the hydration reaction of geopolymer concrete. The binder particles would only partially reacted when the activator

modulus is low, yet excessive alkali modulus beyond the optimum level would attribute over-strongly alkaline which so much so affect the crystallized structure of geopolymer and creating cracks. Deb *et al*. (2014) have investigated the effects of sodium silicate to sodium hydroxide (Na_2SiO_3/NaOH) ratio and alkali activator content on the workability and compressive strength of GGBS-FA blended geopolymer. The Na_2SiO_3/NaOH ratio decreased from 2.5 to 1.5 resulting in increased in compressive strength. Not only that, the strength improved when the activator content increased from 35 % to 40 %, yet reverse effect on the workability. Therefore, the optimal Na2SiO_3/NaOH ratio of 1.5 with 40 % activator content is the optimal alkali activator dosage in terms of strength. However, according to the finding of Salih *et al*. (2014), the compressive strength of POFA-based geopolymer increased by increasing the Na_2SiO_3/NaOH ratio. The Na_2SiO_3/NaOH ratio of 2.5 achieved the maximum strength of 24.48 N/mm^2 at 28 days, yet the strength droved to 23.83 N/mm^2 when Na_2SiO_3/NaOH ratio continue increased to 3.0.

In addition, Singh *et al*. (2016) had further proven the activator-binder ratio of 0.4 developed higher compressive strength than 0.35 activator-binder ratio for blended geopolymer (GGBS-FA). The specimen containing 40 % alkali activator achieved targeted strength of 35 N/mm^2 at 28 days whereas lower strength of 30.26 N/mm^2 is developed by the specimen containing lower activator content (35 %). Besides, the highest compressive strength of FA-GGBS binary blended geopolymer was obtained at optimum activator concentration of 14M due to higher amount of hydrated gels is produced. Activator with lower concentration (12M), would result in insufficient dissolution of aluminosilicate species and therefore geopolymer gel are unable to fully form at this concentration level. However, beyond the optimum concentration, the strength shows decrease trend as

increasing in the activator concentration (16M). This can be explained by viscosity of higher molarity of activator solution limits the leaching of Si and Al as well as might lead to formation of sodium carbonate by reaction between excess Na and atmospheric CO2 (Williamson & Juenger, 2016). Similar outcome has been proven in the studies of Kazemian *et al*. (2015), geopolymer mortar activated by 12 M NaOH developed higher compressive strength at 28 days as above 40 N/mm^2 than which activated by 4 M and 8 M NaOH of below 15 N/mm^2. Besides, increased in Na_2SiO_3 to NaOH ratio from 0.25 to 1.0 contributed to higher strength of 30 N/mm^2 and 40 N/mm^2 respectively. Furthermore, low concentration of alkali activator lead to insufficient dissolution of Si and Al ions, resulted in lower degree of geopolymerization and strength development (Nath *et al*., 2016).

The formula for the specific gravity of combined alkali activator of sodium silicate and sodium hydroxide is provided (Islam *et al*., 2015).

$$\frac{G_{NaOH} \times 1}{1+2.5} + \frac{G_{Na_2SiO_3} \times 2.5}{1+2.5}$$

Moreover, in the research of Al-Majidi *et al.* (2016), positive relationship is found between the silicate modulus (SM) as well as dosage of alkali activator and the compressive strength. In other words, the compressive strength of geopolymer increased with increasing activator dosage and SM. According to Wang *et al.* (2015), the higher dosage of alkaline solutions, the higher the compressive strength. The average compressive strength of binary blended geopolymer concrete (GGBS-FA) with 0.5 % alkaline solution is only 46.61 N/mm^2 at 28 days, yet the average strength increased to 85.09 N/mm^2 and 93.60 N/mm^2 when increasing the alkaline solution to 1.0 % and 1.5 %, respectively. This is because of

Commented [D18]:
Commented [D19]:
Commented [D20]: hg
Commented [D21]:

higher alkaline condition increases the polymerization rate and hydration reaction by providing higher pH value to dissolve and destroy the structure of slag. However, additional content of alkaline solution in geopolymer would shorten the setting time due to accelerating the hardening process with higher rate of polymerization at early stage. Gao *et al*. (2016) had investigated the effect of activator modulus (Ms) namely, SiO_2/Na_2O molar ratio on workability, setting time, compressive strength and porosity of binary blended geopolymer (GGBS-FA). Targeted Ms is achieved by adding appropriate amount of NaOH into Na_2SiO_3 solution. Increased in Ms indicates higher content of sodium silicate in the activator solution. The slump flows are slightly increased from 16.4cm to 23.6 m and 26.5 m with the increase in Ms from 1.0 to 1.4 and then 1.8, respectively. The explanation on this was due to activator solution with higher proportion of Si benefits the workability due to the nature of silicate group. Not only that, increase in activator modulus would extend the initial and final setting time as well.

Commented [D22]:

The activator modulus decreased from 1.8 to 1.0 so does the initial/final setting time reduced from 60/110 min to 26/69 min. The increased in Ms caused relatively higher proportion of Na_2SiO_3 to NaOH in the activator solution, thus prolong the hydration reaction. Next, activator modulus of 1.4 indicates the optimum compressive strength in the study. The compressive strength of 80 % GGBS and 20 % FA blended geopolymer at 7 days increased from 61.8 N/mm^2 to 68.4 N/mm^2 with shifting activator modulus from 1.0 to 1.4 yet lower strength of 65.3 N/mm^2 when beyond 1.4 Ms to 1.8 Ms.

However, contrast finding in the studies of Salih *et al.* (2014), workability of POFA-based geopolymer decrease as the increased in Na_2SiO_3/NaOH ratio. The flow of 243mm for the specimen with 1.0 Na_2SiO_3/NaOH ratio, decreased to 227mm when Na_2SiO_3/NaOH ratio

increased to 3.0. Besides, 2.5 ratio of Na_2SiO_3/NaOH is the optimum ratio of activator in terms of strength development.

2.3.2 Effect of water content

Commented [D23]:

Water performs as the medium in synthesizing the Si and Al during dissolution, condensation and polymerization stages (Xie & Kayali, 2014). Although previous studies have proven reverse effect between the water-binder ratios and compressive strength, yet somehow water content does contribute to higher rate of geopolymerization. According to Kazemian *et al.* (2015), low liquid to solid ratio (L/S) below the optimum point would hinder the strength development of geopolymer mortar. A nearly flat curve movement is observed on the strength development of geopolymer with 0.62 L/S. Higher L/S shows upward movement in the strength development over the curing age. Specimen with 0.81 L/S developed above 30 N/mm^2 compressive strength at 28 days, while the specimen with 0.62 L/S developed strength below 15 N/mm^2. However, excess in liquid might obstruct the strength development as well. Slightly lower strength of 23 N/mm^2 is achieved by the geopolymer mortar with 1.08 L/S compare to 0.8 L/S. Furthermore, Salami *et al.* (2016) had investigated the effect of water content and superplasticizer on compressive strength and workability of 100% POFA-based geopolymer. POFA has high surface area with particle distribution of 1.068µm. This may lead to higher requirement of water to binder ratio for the purpose of desired workability. Three specimens with varying content of water and superplasticizer are studied. The results show highest compressive strength of 18.2 N/mm^2 at 3 days is developed by the specimen with 10 % water content alone, following by around 17.5 N/mm^2 by the specimen with combined 5 % water content and 5% superplasticizer and the lowest compressive strength of about 15 N/mm^2 by the specimen

with 10% superplasticizer alone. The flaw in specimen with superplasticizer alone in terms of strength development is due to weakly bound H-O-H scilicet, weak hydrogen bond in the matrix of geopolymerization products and this is determined by the quantity of H+. According to Xie and Kayali (2014), the higher the water content, the lower the compressive strength of FA-based geopolymer. Increase in water content would dilute the concentrated alkali activator result in lower hydration reaction due to insufficient alkaline strength to dissolve the Si and Al of FA particles. A vast difference is observed between the strength of specimens at 14 days of 16.16 N/mm^2 and 10.81 N/mm^2 with water/binder ratio of 0.22 and 0.26, respectively. Greater proportion of unreacted FA particles is identified in the specimen with higher water/binder ratio. Lower water/binder ratio would accelerate the geopolymerization process. Similar outcome is proven is the studies of Aliabdo *et al.* (2016), compressive strength of approximately 34 N/mm^2 at 7 days is reduced to about 26 N/mm^2 when additional water content of 10 kg/m^3 is increased to 35 kg/m^3. Besides, the water absorption rate and porosity percentage of FA-based increased as the additional water content increased to the specimens.

2.4 Pozzolanic Materials

According to ASTM C 125/C125M (2015), a siliceous or siliceous and aluminous material is alluded to as a pozzolan. This has almost no cementitious potential in itself except for artificially respond with calcium hydroxide in finely isolated structure and within the sight of dampness at standard temperatures to shape compounds with cementitious properties. Pozzolan should be finely isolated and really at that time would silica be able to blend in with calcium hydroxide (fabricated by Portland concrete hydration) with water present to frame strong calcium silicates with cementitious properties. (John & Ding, 2007; Neville,

Commented [D24]:

2011). Report by Duggal (2008), the name pozzolana was gotten from Pozzuoli, a town in an European city, Italy close to Mount Vesuvious on the Sound of Naples. At the point when sand (volcanic residue) from the space was joined with hydrated lime, cementitious properties were found. Pozzolan was blended in with lime to deliver concrete before the appearance of concrete, yet it is as yet used to substitute an extent of concrete in concrete. Moreover, Edmeades & Hewlett (2006), pozzolana has two particular implications. The primary alludes to pyroclastic rocks that are essentially shiny and regularly zeolitized that can be found around Pozzuoli (the antiquated Puteoli of Roman occasions) or around Rome. Genuine and counterfeit pozzolanas are additionally high in silica and alumina, with simply a slight measure of soluble bases (Duggal, 2008). Volcanic magma, pumice, opalineshales, roasted dirt, and fly debris are instances of pozzolanic items. To be responsive, the silica in a pozzolana should be polished or indistinct. Volcanic debris is difficult to the touch, it very well may be red, orange, or dark in shading, and should not break up in water, profoundly rough, marginally destructive, and conducts power when it comes into contact with water. Pozzolanic materials can be ordered into two categories:

Commented [D25]:

i. Artificial pozzolanas

ii Natural pozzolanas

i. Pozzolans are for the most part results of warmth treatment of normal materials, and they are likewise materials with low pozzolanic movement that need extra medicines to accomplish pozzolanic action; they get from substance or underlying modifications of materials that initially had nearly nothing or just gentle pozzolanic properties; they are materials with low pozzolanic action that need extra medicines to accomplish pozzolanic action. (Ramezanianpour, 2014). Fly powder, Impact heater slag, Silica Smoke, Rice Husk

Commented [D26]:

debris, Guinea corn husk debris, and Matakaoline are instances of fake pozzolans, as indicated by Shetty (2009).

ii. Natural pozzolanas has beginning in volcanic, with volcanic ash filling in as the genuine Pozzolan, as indicated by Neville (2011). Normal pozzolans, as indicated by Parhizkar *et al.* (2010), are regular materials containing responsive alumina or silica that have practically no limiting property all alone at the same time, when joined with Portland concrete and as lime is presented to daylight, it sets and solidifies like concrete. Regular pozzolans are partitioned into four gatherings relying upon the presence of the fundamental lime receptive constituent. (Ramezanianpour, 2014). Volcanic tuff and pumice, unaltered volcanic glass, calcined earth or shale, and crude or calcinedopaline silica are the materials being referred to.

2.4.1 Standard specifications and test of pozzolans

According to (ASTM C 618, 2012), pozzolans are divided into diffferent categories;

i. Class N: Regular pozzolans, calcined or crude, that meet the pertinent standards for the class as expressed here, which incorporates certain diatomaceous earths; shales and opalinecherts; calcined or uncalcined tuffs and pumicites or volcanic remains; and different materials, for example, muds and shales, expecting calcination to actuate good properties

ii. Class F: Fly ash shaped by the ignition of bitumious or anthacite coal that consents to the important rules for this class as presented thus.

iii. Class C: The fly ash shaped normally from sub-bituminous or lignite coal that fulfills the important guidelines for this class. This type of fly debris has pozzolanic and notwithstanding pozzolanic properties, cementitious properties exist.

Commented [D27]:

Commented [D28]:

To be delegated pozzolanic, a substance should meet the ASTM C618 (2012) physical and compound details referenced in Tables 2.1 and 2.2.

Tables 2.1 Standard Chemical Requirement

Material contents	Mineral Admixture Class		
	N	F	C
$\Sigma SiO_2 + Al_2O_3 + Fe_2O_3$ min, %	70.0	70.0	50.0
SO_3 max, %	4.0	5.0	5.0
Moisture content	3.0	3.0	3.0
Loss on ignition, max, %	6.0	6.0	6.0

Source: ASTM C 618 (2012)

Tables 2.2: Standard Physical Requirements

Material contents	Mineral Admixture Class		
	N	F	C
Fineness: Amount retained when wet-sieved on 45 μm (No. 325) sieve, max, %	34	34	34
Strength activity index: With Portland cement, at 7 days, min, percent of control	75C	75C	75C
With Portland cement, at 28 days, min, percent of control	75C	75C	75C
Water requirement, max, percent of control	115	105	105
Soundness: Autoclave expansion or contraction, max, %	0.8	0.8	0.8
Uniformity requirements: The density and fineness of individual samples shall not vary from the average established by the ten preceding tests, or by all preceding tests if the number is less than ten, by more than: Density, max variation from average, %	5	5	5
Percent retained on 45-μm (No. 325), max variation, percentage points from average	5	5	5

Source: ASTM C618 (2012)

2.4.2 Pozzolanic activity

As indicated in the work of Duggal (2008), it was reported that when pozzolans are joined with Portland concrete, the free lime consolidates with silica in the pozzolan created during

Commented [D29]:

concrete hydration. The presence of finely partitioned shiny silica and lime causes pozzolanic activity, which brings about the formation of calcium silicate hydrate near that shaped during the hydration of Portland concrete. The silica in the pozzolan responds with the lime framed during Portland concrete hydration, adding to strength development. More hydrated calcium silicate is framed over the long run, which goes about as a folio and fills in the holes, giving impermeability, strength, and always expanding power.

Commented [D30]:

The hydration of Portland cement can be expressed as follows:

$$C_3S + H_2O \longrightarrow \underset{\text{(Calcium silicate hydrate)}}{\text{C-S-H}} + \underset{\text{(Lime)}}{Ca(OH)_2} \qquad (2.1)$$

Equation (2.1) shows how lime from equation (2.1) reacts with silica from pozzolana to form calcium silicate hydrate.

$$Ca(OH)_2 + \underset{\text{(Silica)}}{SiO_2} \longrightarrow \underset{\text{(Calcium silicate hydrate)}}{\text{C-S-H}} \qquad (2.2)$$

The differentiation between dynamic pozzolanas and items with indistinguishable compound piece that have less pozzolanic activity is that formless silica responds with lime more promptly than translucent silica. Since pozzolanic action may just happen within the sight of water, adequate dampness should be made accessible for a lengthy time frame to finish pozzolanic activity. While it is by and large accepted that the lime-silica response is the essential or one in particular that happens, new proof recommends that alumina and iron, if present, likewise take an interest in the substance response. (Dwivedi *et al*., 2006; Duggal, 2008).

2.5 Kaolin

Metakaolin can be described as a dehydroxylated pozzolanic product derived from the high temperature firing of raw kaolin. Kaolin or kaolinite ($Al_2Si_2O_5(OH)_4$) is a clay mineral which contain high amount of layered tetrahedral silicon atom connected via oxygen to octahedral aluminum atom (Peterman *et al.,* 2010). ASTM C 618 (2012) classifies metakaolin as a Class N (or natural) pozzolan. The Meta prefixes attached to kaolin connote change and the change that occurs in this context is the dehydroxylation. Dehydroxylation is the decomposition of kaolinite crystals to a partially disordered structure.

Metakaolin (MK) is unique in that it is not the by-product of an industrial process nor is it entirely natural; it is derived from a naturally occurring mineral and is manufactured specifically for cementing applications. Unlike by-product pozzolans, which can have variable composition, MK is produced under carefully controlled conditions to refine its color, remove inert impurities, and tailor particle size (Brooks & Johari, 2001; Ding & Li (2002). Joseph Davidovits, involved the reaction of fully dehydroxylated kaolinitic clay (known as metakaolinite) with an alkaline silicate solution such as sodium or potassium silicate, or a mixture of both, under strongly alkaline conditions (Davidovits & Davidovics, 1988). Dehydroxylation of kaolinite occurs at temperatures as low as 500–550°C, but the thermal treatment temperature of 800°C recommended in the original.

Commented [D31]:

Many advantages have been reported on the uses of metakaolin as raw material in the synthesis of geopolymer. Some of these advantages include; reduction of efflorescence (a whitish haze which is caused when a calcium hydroxide reacts with carbon dioxide in the atmosphere), increase or boost compressive and flexural strengths, mitigate against chloride

Commented [D32]:

and other permeability, increase resistance to acid attack and durability of the geopolymer (Olawale, 2013). Kaolin can be found in abundance in many parts of Nigeria as shown in Table 1.

Table 2.3: Kaolinitic Clay Deposits in Nigeria

Region	State (Location)	Reserve (MillionTonnes)
North	Kaduna (Mararaban-Rido)	5.5
	Katsina (Kankara, Safana, Malumfashi, Musawa	Very large
	Faskari, Ingawa, Dushin-Ma, Bakori)	Very large
	Kebbi (Illo, Kaoje)	Very large
	Plateau (Major Portar, Nahuta)	8.0
	Borno (Maiduguri)	Large
	Kwara (Lafiagi)	Large
	Bauchi (Darazo, Jagalwa)	18
	Benue (Apa, Iga Okpava, Okpaga)	10
	Niger (Gubaji,Gbako)	very large
South	Anambra (Ogubulu)	4.2
	Enugu (Enugu)	50
	Oyo (Tede)	1.5
	Ogun (Onibode, Ibamaje, Miroko)	large

Source: Ojo *et al.* (2017).

2.6 Cassava Peel Ash

Building materials account for between 40-60% of the total construction cost (Ayangade *et al.*, 2004), and this is attributed to the fact that basic conventional building materials like cement and aggregates are becoming increasingly expensive due to high cost incurred in their processes, production and transportation. Cassava is known to be a major source of carbohydrates with Africa being the largest centre of production. Adesanya *et al.* (2008) reported that cassava peel constitutes between 20-35% of the weight of tuber, especially in the case of hand peeling. Based on 20% estimate, about 6.8 million tonnes of cassava peel is generated annually and 12 million tonnes is expected to be produced in the year 2020. Indiscriminate disposal of cassava peels due to gross underutilization as well as lack of appropriate technology to recycle them is a major challenge, which results in environmental

problem. These wastes would even be more problematic in future with increased industrial production of cassava products such as cassava flour and garri. In the same vein, developing nations of the world are challenged with issues of managing domestic and agricultural wastes as a result of the attendant growth in population and increasing urbanization. Reuse of these wastes provide an attractive option that promotes savings and conservation of natural resources from further depletion hence creating a sustainable environment. Thus, there is need to search for alternative methods to recycle cassava peels. Cassava peels burnt at controlled or uncontrolled temperature showed that its ash possessed an appreciable quantity of silica and alumina for use as pozzolan in concrete (Olonade & Mohammed, 2019). According to (Salau & Olonade. 2011), the pozzolanic potential of cassava peel ash (CPA) and their results showed that cassava peel ash possesses pozzolanic reactivity when it is calcined at 700^0C for 90 minutes. At these conditions, CPA contained more than 70 per cent of combined silica, alumina and ferric oxide.

Commented [D33]:

2.7 Rice Husk Ash

Global production of rice was estimated to be around 600m tons per year, majorly of which is grown in Asia (Younes, 2018). The milling process of rice crops generates a byproduct commonly referred to as rice husk, which is the hard-protecting covering of grains of rice. Rice husk ash is obtained from the combustion of rice husk in the boiler, which is collected from the particulate collection equipment located upstream to the stack of rice–fired boilers (Naiya *et al.,*2009). Prior to the combustion process, rice husk constituted 75 – 80% organic substance, and 15 – 20% of inorganic substance. The burning is an effective way of removing the organic substance while generating energy, leaving behind inorganic ash majorly consisting of Silica (Kanth & Muthu, 2015).

Based on the research conducted by (Kosnatha, 2007), the result indicated that the pozzolanic activity in rice husk ash depends on the amorphous silica content, the particle size distribution, and its specific surface area. The work of Nair *et al.,* (2008) shows that the rice husk combustion of 500°C-700°C produces maximum silica content. It has higher pozzolanic activity than silica form (Saloma *et al.,* 2016). Never the less high pozzolanic in rice husk ash can lead to enhanced hydration reactions, increased large-age strength, reduced porosity, and improved durability (Sreevidya *et al*., 2012; Taylor, 1997). Owing to these facts, rice husk ash is being considered as one of the most important pozzolanic materials with improved characteristics of the hardened blended geopolymer mortar.

2.8 Sustainability and Environmental Benefits

Carbondioxide (CO_2) discharges from OPC creation went from 5% to 10% of all out-ozone depleting substance (GHG) outflows in the environment (Obada *et al.,* 2008). Subsequently, the World Business Chamber for Supportable Turn of events (WBCSD) proposed in 2002 that CO_2 outflows from concrete assembling tasks be decreased by 30% by 2020 and 60% by 2050. Concrete creation is plainly unreasonable at these measures of CO_2 contamination. These contamination issues are genuine; for each huge load of Portland concrete made, 1 to 1.25 huge loads of CO_2 is radiated into the environment by consuming carbon. Therefore, lessening OPC request diminishes CO_2 contamination into the air from concrete handling. Therefore, bringing down the OPC in concrete blends would bring about critical decreases in (GHG) discharges. Due to the huge measure of cement utilized every day all throughout the planet, the maintainability hypothesis for the utilization of Supplementary Cementitious Materials (SCMs, for example, pumice is that regardless of whether there is a slight decrease in OPC in concrete utilizations per ton of cement made,

the subsequent ecological advantages are high (Altwair & Kabir, 2010). Accordingly, supplanting some measure of OPC brings CO_2 outflows down to the climate straightforwardly. Because of the use of SCMs, the weight of green gas outflows from cement calcinations can be decreased.

2.9 Effects of Pozzolan on Engineering Properties of Geopolymer Concrete

The engineering properties of geopolymer at room temperature are influenced by the different composition of binder among RHA, CPA and MK. In this study, the engineering properties of ternary blended geopolymer mortar to be studied are including compressive strength, density, sulphate resistant, acid resistant and chloride resistant.

2.9.1 Compressive strength of geopolymer

The compressive strength of binary or ternary geopolymer is vastly influenced by the composition of binder. Variation in the composition of binder (RHA-CPA-MK) would cause varying in Si/Al ratio, Ca/Si ratio and Na/Si ratio which are directly affects the properties and performance of geopolymer concrete. Zhou *et al.* (2016) had investigated the effect of variation in Si/Al ratio and on compressive strength at both low-Al and high-Al FA-based geopolymer. Result indicates optimum Si/Al ratio of 2.0 developed highest 7 days compressive strength of 21.5 N/mm^2 at room temperature (20^{o}C), following by Si/Al ratio of 2.5 and then 1.5. The compressive strength dropped dramatically to 11 N/mm^2, when Al content is greater than Si with Si/Al of 1:1.15. Besides, all of these specimens with different in Si/Al ratio, continuously increased the strength when under heat curing up to 80^{o}C.

Yusuf *et al.* (2014) postulated that the optimum ratio of 20% RHA and 80% CPA found to be highest compressive strength of 44.57 N/mm^2 at 28 days, beyond 20 % of RHA resulted

Commented [D34]:

Commented [D35]:

Commented [D36]:

Commented [D37]:

in drawback effect in terms of compressive strength development. However, in the studies of Salih *et al.* (2015), it was discovered that the addition of RHA in the mix from 10% up to 50% increased the strength at all ages, even beyond 20%. The equal ratio of RHA and CPA developed the highest strength at 28 days of 78.12 N/mm^2 compared to 0 % of RHA specimen with the strength of 31.04 N/mm^2 at 28 days. The inclusion of RHA contributes to acceleration of hardening process, thus reducing the setting time of the mix. Furthermore, Islam *et al*. (2015) had found that the finer the particles size of CPA, the higher the compressive strength due to better filler effect, yet might affect the workability of the mix.

Commented [D38]:

However, the addition of RHA improved the initial strength at early stage and this could facilitate the reuse of formwork and hasten the construction. Soutsos *et al*. (2016) had investigated the linear relationship between the compressive strength at 1, 7 and 28 days with the amount of RHA in geopolymer which were cured at room temperature. Significant increase in compressive strength was observed from 20 to 50 N/mm^2 with only 20% of RHA is added. Curing temperature is the essential factor of strength development in FA based geopolymer. Besides, the highest compressive strength of 80 N/mm^2 was achieved at 28 days for mortar consist of 80% RHA and 20% MK at room temperature. Similar phenomena were observed in the research of Puligilla and Mondal (2013), RHA contributes to higher compressive strength at room temperature and hasten the setting time of geopolymer. The presence of soluble calcium dissolved from RHA accelerates the hardening of geopolymer. Not only that, higher final strength is achieved with greater content of GGBS due to higher rate of geopolymerization of both MK and RHA particles. Gao *et al.* (2015) had investigated the effect of incorporation of nano-silica in RHA-MK

blended geopolymer concrete. The nano-silica composes essentially of SiO_2 (98.68 %), which could be assumed as similar effect for blending CPA into RHA-MK binary blended geopolymer concrete as CPA consists mainly of Si (63.41%) too. Increased in nano-silicate content enhanced the compressive strength up to optimum ratio of 2% and 6.4% increment in strength when nano-silicate content increased from 0% to 1%, but the strength dropped when nano-silicate content reached 3%. Besides, increased in nano-silicate content resulting slightly delay the initial and final setting times.

In addition, Deb *et al.* (2014) investigated the effects of GGBS content, sodium silicate to sodium hydroxide (Na_2SiO_3/NaOH) ratio and alkali activator content on the compressive strength of RHA-MK blended geopolymer. The compressive strength of geopolymer increased at higher content of RHA and activator but lower Na_2SiO_3/NaOH ratio of 1.5. The optimum 28 days compressive strength of 51 N/mm^2 was achieved by the geopolymer containing 80% of MK and 20% of RHA in the binder and 40% of activator content with 1.5 Na_2SiO_3 to NaOH ratio. Furthermore, inclusion of RHA in MK-based geopolymer from 10% to 50% increased the compressive strength at ambient curing from 18.45 to 45 N/mm^2 at 28 days with the cost of accelerated hardening and resulting dramatically reduction in setting time as well as high rate of dry shrinkage (Al-Majidi *et al*., 2016). Next, in the studies of Wang *et al.* (2015), increase in the FA replacement in RHA-MK blended geopolymer could bring drawback effect on compressive strength. The greater the replacement of MK the lower the compressive strength at all ages as well as all level of alkaline solutions. The optimal compressive strength of 93.06 N/mm^2 is 100 % RHA with 1.5 % alkaline solution at 28 days. Furthermore, similar results are proven by Gao *et al.* (2016), the addition in RHA content contributed to development of higher compressive

strength at all ages. The compressive strength specimen with the RHA/MK ratio of 40/60 at 7 days with activator modulus of 1.4 is 58.4 N/mm^2. It slightly increased to 62.6 and 68.4 N/mm^2 when increasing the RHA proportion to 60% and 80%, respectively. Besides, the compressive strength of geopolymer is very sensitive to curing period, curing temperature, water/binder ratio and alkaline condition as well. The effect of different curing methods including bath curing, sealed curing and exposed curing with varying water-binder ratio of 0.33, 0.45 and 0.5 on the compressive strength of RHA based geopolymer has been investigated by Collins and Sanjayan (2008). First for the bath curing, specimens are immersed in saturated lime water at 23ºC and specimens are stored in confined space at 23ºC for sealed curing.

Lastly, exposed curing is exposing the specimens at 50% relative humidity (RH) at 23ºC. Results have shown bath curing achieved highest compressive strength despite of shifting the water/binder ratio to all level. In the contrast, exposed curing indicates a decrease trend on compressive strength and developed un-ideal and lowest strength with all level of water contents. Furthermore, in the research of Xie and Kayali (2014) a positive relationship between compressive strength development of MK-based geopolymer and curing period is observed. Compressive strength of 3.54 N/mm^2 at 7 days is subsequently increased to 16.16 N/mm^2 at 14 days. Besides, heat curing could hasten the strength development as well. Specimen with 4 hours elevated temperature curing achieved strength of 15.71 N/mm^2 is then increased to 42.07 N/mm^2 when subject to 24 hours heat curing. The compressive strength of MK-based geopolymer with 4 hours heat curing is comparable to specimen cured at 7 days. This indicates the important of elevated temperature to MK-based

geopolymer during the early stage of curing period. Continuous heat curing over 24 hours would bring on-site effect to strength development of geopolymer.

2.9.2 Density of geopolymer

Commented [D39]:

The measurement of density could indirectly provide an insight to the degree of geopolymerization, presence of voids or porous structure, degree of compactness and compressive strength of geopolymer. Yong *et al*. (2016) investigated the effect of changes in density on the compressive strength and pore structures. Form concrete is a ventilation technique by used of lightweight concrete with high degree of voice space (Zhang *et al*., 2014). In this research, specific volume of foam is added into specimens with density of 1300 and 1500 kg/m^3 respectively. The difference between foam added specimens resulting in reduction in density and normal dense geopolymer is observed. The reduction in density shows decrease trend of compressive strength and an upward trend of pore structure as well as water absorption rate in the MK-CPA blended geopolymer. The compressive strength of formed geopolymer with density of 1300 kg/m^3 at 28 days was 8.3 N/mm^2, yet compressive strength of 13.5 N/mm^2 was developed by the formed geopolymer with higher density of 1500 kg/m^3.

Hence, it explicitly illustrated the positive correlation between density and compressive strength. Xie and Kayali (2014) also investigated a decreasing trend in density of FA-based geopolymer over the curing period. The density of 1.77 g/cm^3 is measured for the specimen cured at room temperature at 7 days, subsequently decreased to 1.75 g/cm^3 at 14 days ages. Similar trend is observed when FA-based geopolymer is subjected to heat curing. Density of 1.7 g/cm^3 with 4 hours heat curing is then reduced to 1.69 g/cm^3 after 24 hours of heat curing. Besides, water content is adversely affected the density of geopolymer. Lower

density of is measured for the specimen with 0.22 water/binder ratio compared to specimen with higher water/binder ratio of 0.26 in all condition. However, in this case, reduction in density does not indicating lower compressive strength. The reduction of density over curing period is merely due to evaporation of internal moisture. The higher solid to liquid (S/L) ratio, the higher the density of POFA-based geopolymer paste (Salih *et al*., 2014). Result has shown variation in the density of 1798.0 kg/m^3 and 1722.4 kg/m^3 with different in S/L ratio of 1.32 and 1.0 respectively. Higher density is obtained on the specimen with higher S/L ratio due to greater amount of binder lead to more compact structure and little porous voids with greater amount of reacted products.

Commented [D40]:

Furthermore, Cheah *et al.* (2016) also reported that the increase in the replacement level of GGBS from 72% to 80% in RHA-MK binary blended geopolymer mortar resulted in an upward trending of bulk density from 2182 kg/m^3 to 2236 kg/m^3 at 90 days. This is mainly due to denser microstructure was produced in the specimen with higher content of RHA inclusion.

Commented [D41]:

Furthermore, with reference to the studies of Islam *et al.* (2014) and Alanazi *et al*. (2016), fully RHA-based geopolymer developed highest oven-dried density of 2163 kg/m^3 at 3 days; loose to completely MK-based geopolymer which found to be lowest 3-day oven-dried density of 2014 kg/m^3. The variance in density was much influenced by the specific gravity and fineness of pozzolanic binders. Besides that, the density could be determined by the filling effect of particles into the voids. CPA has relatively coarser particles as compared to RHA and MK. Hence, the finer particles of RHA contributed to enhance its density of about 7.5% as compared to CPA-based geopolymer mortar.

2.10 Durability in Concrete Structures

Structural durability according to the literature (ACI, 2001; Yip *et al.*, 2005; Yao *et al*., 2009; Temuujin *et al.*, 2010b; Soylev & Ozturan, 2014; Suksiripattanapong *et al.*, 2015; Wang *et al*., 2015) means the structure's lifetime with efficient serviceability. In the past, engineers and designers considered the compressive strength of concrete as the only factor which is effective in the quality and durability of structures. However, environmental conditions can act as an effective factor in quality and an efficient lifetime of structures. In other words, in a destructive environmental condition, the concrete hurts in a shorter period than regular useful service life. Premature failures in the structures as a result of destructive environmental conditions could be considered as meaningful evidence for the necessity of concrete durability. This issue in infrastructures like dams, tunnels, bridges, or power plants, which need to have a long service life and with the expensive cost of repair and maintenance, bolds as particular importance. Although, concretes with high compressive strength regularly have higher resistance against physical and chemical attacks in destructive environments, the other factors such as permeability and congestion in concrete can directly affect the durability and quality of concrete (Phoo-ngernkham *et al.*, 2015; Nath *et al*., 2015a; Rostami, 2015; Nath *et al*., 2015b). Generally, concrete destructive factors can be categorized in external and internal factors.

External factors such as:

1) Physical factors: Freeze/thaw cycle, temperature changes, humidity percentage
2) Chemical factors: Sulphate attacks, acidic attacks, carbonation
3) Mechanical factors: Abrasion, erosion, spoilage in hydraulic structures

Internal factors such as:

1) Alkaline reactions in aggregates
2) Existence of minerals in concrete components
3) Permeability of concrete (ACI Committee, 2001).

2.10.1 Sulphate attack

The chemical reactions between sulphate ions and cement hydration productions are called sulfate attack, which can directly threaten the durability of concrete in aggressive environments. Sulphate ions could be found in the sea, groundwater, soil, and waste water (El-Hachem *et al.*, 2012). The reactions mentioned above could lead to crack, crush, softening, expanding, and weakness in the strength of concrete (Monteiro & Kurtis, 2003). Sulphate attacks are categorized into two main groups:

A. Internal sulphate attack (ISA)

Internal sulfate attack occurs when the amount of sulphate in concrete components like cement, aggregate, chemical admixtures, or water significantly increases. The internal sulfate attack leads to:

- Delayed ettringite formation (DEF): the formation of ettringites after the concrete becomes hardened, causes expansion and results in cracking in the concrete.
- Decomposition and deformation of ettringites and as a result unsuitable condition in the curing process
- Increasing the deformation of ettringites results in increasing cracks and making free spaces around aggregates (Collepardi, 2003).

B. **External sulphate attack (ESA):**

External sulphate attack is a result of the chemical reaction between cement paste and the sulfates existing in the soil. This chemical reaction could be a consequence of high

permeability in the concrete and high level of moisture and sulphates in the soil. Moreover, External sulphate attack leads to cracking, crushing, and weakness in compressive strength. This sulfate attack can be as a result of chemical reactions below:

C. Sulphates in reaction with hydroxide calcium (CH) and cement paste (C-S-H), forms gypsum:

$$CH + C - S - H + SO_4^{2-} + H_2O \longrightarrow CSH_2$$

Which S means SO_2^{-4} (Collepardi, 2001). As presented in chemical equation below, the existence of sodium sulfate in adjacent of calcium hydroxide in the concrete generates magnesium hydroxide and gypsum:

$$Ca(OH)_2 + MgSO_4 + 2H_2O \longrightarrow CaSO_4 \cdot 2H_2O + Mg(OH)_2.$$

An investigation on concrete specimens adjacent to magnesium sulfate. They saw a layer of magnesium hydroxide forms on the specimen's surface immediately after the existence of magnesium sulfate (Santhanam *et al.*, 2002). In the case of the existence of magnesium sulfate ions, the chemical reaction above continues until all calcium hydroxides existing in the concrete changes to calcium sulfates. Reduction in calcium hydroxide results in a reduction in PH-value. Moreover, the durability of the cement gel is depended on the presence of calcium hydroxide. Thus, some parts of the cement gel should be decomposed to produce some calcium hydroxide and increase the PH-value. In conclusion, this procedure leads to decomposing the cement gel and weakness in concrete strength (Santhanam *et al.*, 2002).

Among various types of sulphates, such as magnesium sulphate, sodium sulphate and calcium sulphate. Sodium sulphate has the most destructive effects on the concrete.

- Sulfate attacks to calcium aluminate hydrates $C - A - H$ and $C_3A.CS_{12-18}$

$$C_3A{\cdot}CS_{12-18}C-A-H + SO_4^{2-}\cdot 2\,H_2O + H_2O \longrightarrow C_3A{\cdot}CSH_{32}$$

In this reaction, ettringite is generated, which expands and results in cracking and crushing in the concrete.

- The reaction below illustrates how thymocytes generate as a result of sulfate attack to calcium hydroxide (CH) and cement gel:

$$CH + C-S-H + SO_4^{2-} + CO_3^{2-} + H_2O \longrightarrow CS\cdot CS\cdot CCH_{15}$$

The existence of thymocytes results in compressive and bond strength and can also lead to the softening of concrete. This reaction occurs in high humidity and low temperature (Puertas *et al.*, 2002). Research in 2002 on the chemical resistance of alkali-activated slag mortars with various kinds of activators proved that sulfate resistance of these mortars is depended on the nature of activator, which is used in the mix design. Slag mortars that are activated with sodium hydroxide due to their high ratio of Ca to Si in comparison with slag mortars, which are activated with sodium silicate, are more sensitive to sulfate attack (Puertas *et al.*, 2002). Bakharev *et al.*, (2002) investigated alkali-activated slag concrete in the condition of sulphate attack with ASTM C 1012 (2019) standard. These specimens were immersed in 5% sodium sulphate solution and 5% magnesium sulphate solution for 12 months, the same condition was applied on an OPC concrete but for 60 days. Figures 2.1 and 2.2 illustrates that the strength development was the same in both environments. However, after that, weakness in strength was more significant in OPC in comparison with alkali-activated slag concrete. After 12 months in sodium sulphate, the alkali-activated slag concrete had a 17% weakness in strength; however, in OPC, this weakness development was about 25%. In magnesium sulphate after 12 months, the weakness for alkali-activated slag concrete was about 23%, but OPC concrete was about 37% of initial strength. As

mentioned above, OPC concrete in the existence of sodium sulphate generates ettringite. These specimens in the existence of magnesium sulfate generate ettringite in addition to gypsum. Alkali activated slag specimens with adjacent of sodium sulphate, were out of ettringite or gypsum. However, these specimens adjacent to magnesium sulfate produced gypsum. The generated gypsum causes cracks on the edges of specimens. It leads to the softening of concrete in the existence of magnesium sulfate (Bakharev *et al.,* 2002).

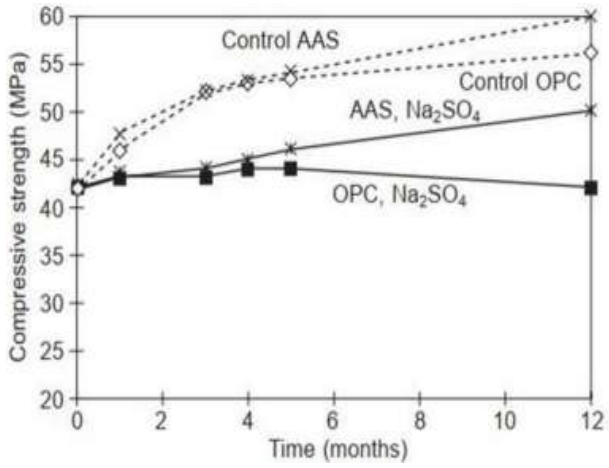

Figure 2.1: Compressive strength in the OPC and AAS specimens exposed to the sodium sulphate solution (Bakharev *et al.,* 2002).

Rodriguez and his team in 2008 made an investigation on sulfate resistance of alkaliactivated slag concrete and OPC concrete. Their results proved that after 90 days, the compressive strength of alkali-activated slag concrete, which was in adjacent to 5% sodium sulfate solution, remains constant as oppose to OPC concrete in which the compressive strength drops for about 43% in same conditions (Rodríguez *et al.,* 2008). Komljenovic *et al.* (2013) studied on alkali-activated slag concrete in comparison with binders that are

made of slag and cement. They showed that alkali-activated slag concrete has more resistance against 5% sodium sulfate solution (Komljenović *et al*., 2013). Alkali-activated slag concrete, which is activated with sodium silicate after 180 days in adjacent to 5% sodium sulfate are more durable in comparison with OPC concretes (Heikal *et al*., 2014). A study on the effect of sulphate environments on concretes, which consist of micro silica, slag, and limestone powder showed that when he substituted cement with 10% of micro silica, the resistance of concrete against magnesium sulfate environments reduced (Mostofinejad *et al*., 2016). Cho *et al*. (2018) investigated alkali-activated geopolymer mortars based on fly ash and slag in two environments, such as sodium sulphate and magnesium sulphate. They used sodium hydroxide and sodium silicate solutions where slag was substituted with fly ash in 0, 30, and 50%. The curing process took 24 hours at 23 and 70. After warm curing, they immersed the specimens at 23 constant and 60% of moisture for 28 days Figures 2.6 and 2.7, show the increment in the mass of specimens depends on the type of sulfate solution where the specimen is immersed. The most increment in the mass of specimen was 1.8% in sodium sulphate solution, which is for the specimen with 100% of fly ash. On the other side, with increasing the proportion of slag, the increment in mass decreased, and in magnesium sulphate solution, increasing the proportion of slag results in increasing the mass.

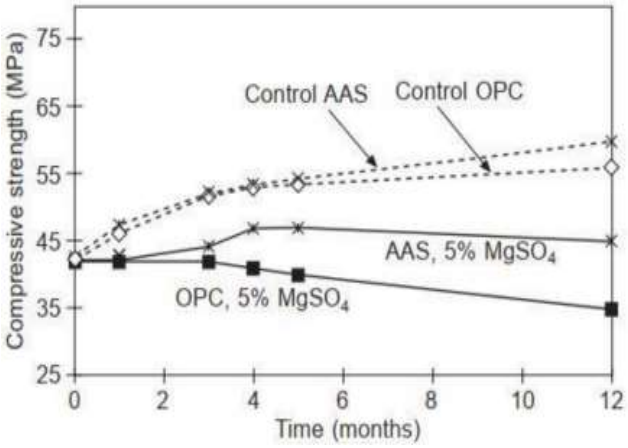

Figure 2.2: Compressive strength in the OPC and AAS specimens exposed to the sodium magnesium solution (Bakharev *et al*., 2002).

Figures 2.3 and 2.4 shows that increasing the proportion of slag in sodium sulphate environment results in increasing compressive strength as oppose to a magnesium sulphate environment, which drops the compressive strength in the specimens. Increasing the mass and decreasing in the compressive strength in magnesium sulfate solution is a result of forming gypsum and brucite in the chemical reactions (Cho *et al.*, 2018).

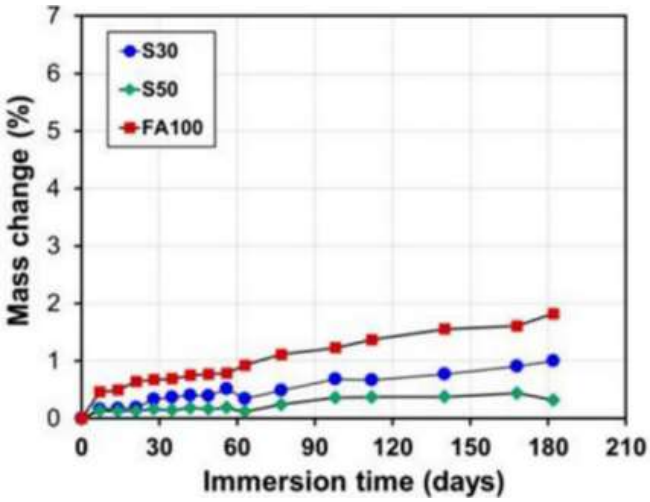

Figure 2.3: Specimens exposed to the magnesium sulphate solution (Cho *et al*., 2018)

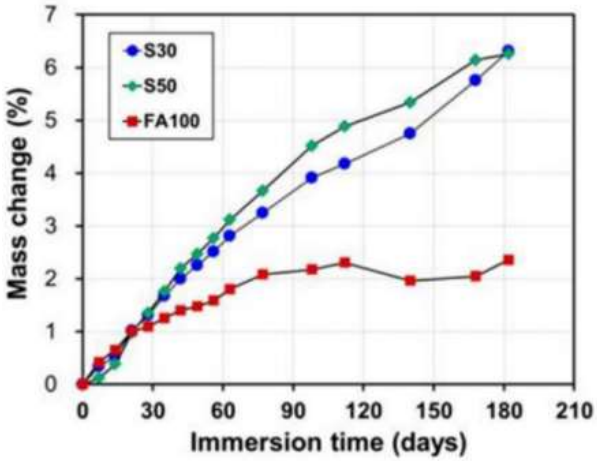

Figure 2.4 Specimens exposed to the sodium sulphate solution

2.10.2 Acidic attack

Concrete structures are commonly adjacent to groundwater, industrial waste water, and acidic rains. Thus, acidic resistance of concrete could be an essential characteristic that affects its performance in practice (Deb *et al.,* 2016). OPC concrete cannot perform acceptable behavior in acidic environments (ACI Committee, 2001). Besides, the aggressive acids which are exposed to the concrete are in a wide range of variety. All acidic solutions have PH-value under seven and they are also categorized in organic (weak acids) and mineral acids. Nitric acid (HNO_3), Hydrochloric acid (HCL) and sulfuric acid (H_2SO4) are the primary mineral acids that are so dangerous for concrete and can directly affect the durability of concrete (Mellado *et al.,* 2017). Sulfuric acid is one of the most harmful acids as it can affect the concrete as both acidic and sulphate aspect of its characteristics which can double the problem. Destruction of sewage concrete pipes due to sulphuric acid attack is a global problem (De Vargas *et al*., 2011; Garcia-Lodeiro *et al.,* 2011; Barbhuiya & Kumala, 2017). The chemical reactions below illustrate how corrosion happens in concrete in the existence of sulfuric acid:

$$Ca(OH)^2 + H_2SO_4 \longrightarrow Ca\ SO_4 \cdot 2\ H_2O,$$

$$CaSiO_2 \cdot 2\ H_2O + H_2SO_4 \longrightarrow CaSO_4 + Si(OH)_4 + H_2O,$$

$$3CaO{\cdot}Al_2O_3{\cdot}12H_2O + 3(CaSO_4{\cdot}2H_2O) + 14H2O \longrightarrow 3CaO{\cdot}Al_2O_3{\cdot}3CaSO_4{\cdot}32H_2O$$

Gypsum as the first production of this reaction forms on the surface of concrete it can result in tension stress and cracking in the concrete. This layer of gypsum can cover the surface of concrete and reduce the corrosion speed (Hardjito *et al.,* 2005; Bassuoni & Nehdi, 2007; Hu *et al.,* 2008). On the other hand, this gypsum on the concrete can react with calcium aluminate and generate ettringite, which leads to an increment in volume up to 7 times in

gypsum. It can lead to forming micro and macro cracks in the concrete (Monteny *et al*., 2000). Bakharev *et al*. (2003) studied on corrosive effects of acetic acid solution (PH=4) on alkali-activated slag concrete, and OPC concretes. The results showed a weakness in the compressive strength of about 47% in OPC specimens and 33% in alkali-activated slag specimens after immersion in an acidic solution for 12 months in comparison with immersed specimens in the water. It proves that alkali-activated slag concrete restrains better against acidic attacks in comparison with OPC concrete. This result is because of a smaller ratio of Ca to Si in slag paste (Bakharev *et al.*, 2003). Allahverdi and Skavara (2005) studied the resistance of binders with fly ash and activated slag against acidic corrosion has been done. In this study, after 28 days of curing, the pastes were immersed in sulfuric acid with different PH. The alkali-activated slag and fly ash in the acidic environment with PH=1, formed a crushed and hardened corroded layer. In the environment with PH=2, this corroded layer was stiffer with tiny cracks.

In the environment with PH=3, a soft layer formed, which can be removed easily. Researchers checked the specimen after curing in the environment with PH=2 under the microscope, and they saw gypsum crystals in the corroded layer (Allahverdi & Skvara, 2006; Allahverdi & Skvara, 2005) The researchers concluded that the deposited gypsum in the corroded layer leads to covering the concrete and disturb the destruction process with acidic solution (Pacheco-Torgal *et al.*, 2014). Bernal *et al.* (2012) and his team made another investigation on the resistance of alkaliactivated slag mortars and OPC mortars against acidic attack. They made specimens and immersed them in hydrochloric acids, nitric acids, and sulfuric acid solution with PH=2. They found an insignificant change in the strength of alkali-activated slag mortars in the existence of mineral acids. A noticeable

increase in compressive strength in adjacent of nitric and sulfuric (Bernal *et al*., (2012). Granero *et al.* (2016) carried out experiments on the durability of alkali-activated material against sulfuric acid. The alkali-activated material was GGBFS and type F fly ash. They also used OPC as a reference mix design. In OPC specimens, they saw a reduction in both mass and size; however, in alkali-activated slag specimens, they saw an increment in both mass and size. They also saw the formation of gypsum as a corrosion production in both OPC and alkali-activated slag. Besides, there was nothing changed noticeably in the mass and size of alkali-activated fly ash specimens (Aliques-Granero *et al*., 2017).

Rao and Madhuri (2018) used a composition of sodium silicate and sodium hydroxide for activating slag in alkali-activated slag concrete and studied on their resistance against sulfuric acid in comparison with OPC concrete. As a result, mass reduction and permeability were significantly lower than OPC specimens. On the other hand, alkali-activated slag specimens showed less weakness in compressive strength in comparison with OPC concrete.

2.10.3 Permeability

The resistance that a concrete show against external destruction factors such as water, air, chemicals with high and low PH-value, external gases such as corrosive or non-corrosive, is called the impermeability of concrete. As these factors are external, but they need to penetrate the concrete to act as an effective attack. Thus, permeability is considered a noticeable factor in the durability of concrete. Concrete is known as a permeable and porous material. On the other side, water as the most crucial solution which exists in most chemical reactions is considered as a significant destructive factor for permeable materials. Tiny pores and internal cavities are called the porosity of a material, which is commonly

calculated as a percentage of the total volume of the concrete (Wilson & Ding, 2007; Mirza *et al*., 2014; Lim *et al*., 2015; Behfarnia & Shahbaz, 2018). The porosity of concrete and the carbonation around the rebars can make the reinforcement sensitive to corrosion with the existence of chloric ion (Pacheco-Torgal *et al*., 2008a; Pacheco-Torgal *et al*., 2008b; Arbi *et al*., 2016; Ojo *et al*., 2017). The carbonation process is a result of CO_2 penetration as a negative factor for concrete. A tiny layer of oxide covers the external surface of the concrete, which prevent corrosion. This layer remains even in high alkaline environments (PH=13). However, during carbonation, this PH-value reduces to less than nine and simplifies the corrosion process of reinforcement (Mohamed, 2019). The carbonation is a result of the chemical reaction between CO_2 and water. This reaction produces carbonic acid. Then, this weak acid reacts with productions from hydration and reduces the alkaline of concrete (Behfarnia & Rostami, 2017). This chemical reaction is demonstrated below:

$$CO_2 + H_2O \longrightarrow H_2CO_3$$

$$Ca(OH)_2 + H_2CO_3 \longrightarrow CaCO_3 + 2\,H_2O$$

$$C - S - H + H_2CO_3 \longrightarrow CaCO_3 + SiO_2 \cdot nH_2O$$

The most effective factor in rustiness and corrosion in concrete is the chloride ions. These ions can exist in aggregates or admixtures or external mater like seawater. For activating the corrosion process in rebar, the concentration of chloride ion must exceed the allowable amount. The required concentration of chloride ion for activating the corrosion process depends on the PH-value in the cement paste. The corrosion can even begin without the existence of chloride ion in the PH-value of less than 11.5. However, for PH-value of higher than 11.5, the existence of chloride ion is necessary. When the amount of chloride ion exceeds the allowable concentration, the protective layer on the rebar disappears. In the

next step, the iron ions react with chloride ions and produce $FeCl_2$. This product reacts with water and changes to unstable hydrochloric acid. The unstable acid leads to decreasing PH-value and decomposes to chloride ions. Furthermore, the produced chloride ions repeat this procedure to making a loop, which leads to the corrosion of rebars (Bondar *et al*., 2018). An investigation by Chengning, (1993) proves that the characteristics and structure of alkali-activated concrete depend on the characteristics of the alkali activator.

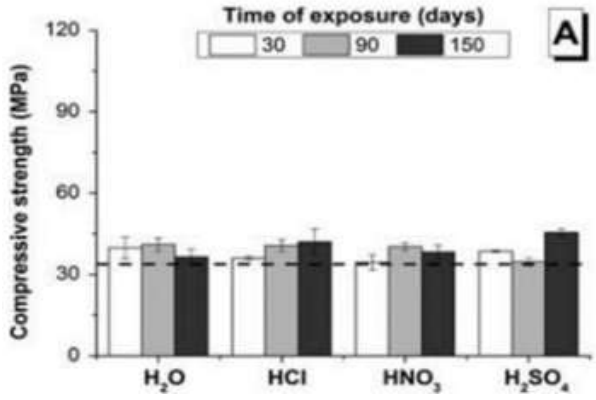

Figure 2.5: Compressive strength of OPC mortars (Bernal *et al*., 2012).

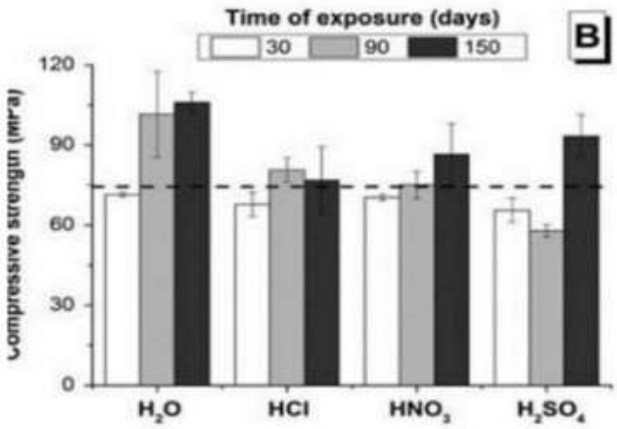

Figure 2.6: Compressive strength of AAM mortars (Bernal *et al*., 2012).

CHAPTER THREE

3.0 MATERIALS AND METHODS

3.1 Materials

The materials used in the test programme includes Portland cement (CEM 1), Rice Husk Ash (RHA), Metakaolin, Cassava Peel Ash (CPA), fine aggregate, Alkaline solution (Sodium Silicate (Na_2SiO_3) and Sodium Hydroxide (NaOH)), water and superplasticizer.

Commented [D42]:

3.1.1 Cement

Portland Cement type CEM II/A-LL, 42.5 N from Dangote Cement Company conforming to BS EN 197-1 (2011) and NIS 444-1 (2003) was used as main binder (PC) throughout the investigation. The cement was obtained from local cement merchant in Minna and effort was made to ensure that the supply is gotten from the most recent stock and kept in dry position.

3.1.2 Supplementary cementitious materials

Commented [D43]:

The rice husk used in this research work was collected from a local mill in Minna, Niger State and the RHA was obtained from rice husk through calcination at a temperature of about 600-700^{o}C in a controlled environment then pulverized using a grinding mill machine and incorporated at different varying proportions as shown in Table 3.1. The RHA powder was white in colour, which was an indication of complete burning of all carbon and impurities within the husk. The CPA used in this study was gotten from dried Cassava peel calcinated at 750°C in an electrical furnace for 2 hours and it is dark ash in colour. The specific gravity of CPA is 2.3. The Cassava peel was collected as a waste material

generated from cassava plant from Doko village in Lavun LGA of Niger state. The MK sample used was produced in the laboratory by the calcination of earth explored kaolin, sourced from Alkaleri Local Government of Bauchi State, Nigeria. The calcination was performed at 750^{o}C in an electrical furnace for 2 hours, yielding calcined kaolin clay or MK with specific gravity of 2.2 after which the sample was grinded to 75 micrometers. MK has a distinctive off-white colour close to that of the parent kaolin. The appearance of kaolin has changed from pure white to floral whitish after dehydrocyclization process.

Commented [D44]:

The powdered PC, MK, CPA and RHA were then packaged and sent to Rolab research and diagonistic laboratory Ibadan, for X-Ray Florescence (XRF) analysis to determine their oxide composition.

3.1.3 Fine aggregate

River sharp sand with maximum size of 4.75 mm was used in this study. The sand was used at saturated surface dry conditions and its grading was measured according to ASTM C33/C33M (2019).

Commented [D45]:

3.1.4 Superplasticizer

Master Rheobuild plasticizer of polycarboxylic ether (PCE) polymer based Superplasticizer supplied by BASF Nigeria Limited. Master Rheobuild plasticizer was used as a high range water reducer and was administered at constant concentration of 10% by weight of binder.

3.1.5 Water

Clean potable water as specified by BS EN 1008 (2015) available within the concrete laboratory of Department of Building, School of Environmental Technology, Federal

University of Technology, Minna was used for mixing.

Commented [D46]:

3.2 Methods

The work was mainly experimental and the approach adopted for the study is discussed under the following sub-heads; experimental plan, material analysis (Physical and Chemical), Mechanical properties (Compressive) and Durability properties.

3.2.1 Experimental plan

The study implemented the following experimental procedures in actualizing the study objectives as outlined in section 1.3 and thus fits into work plans with the details provided in the following subsections:

3.2.1.1 Work plan one

This is in line with objective one (1), which is concerned with determining the physical and chemical properties of RHA, CPA and MK constituents to develop a mixture proportion of ternary synthesized geopolymer mortars with enhanced durability. Procedure for determining the physical properties of the aggregate used was also discussed therein.

3.2.1.2 Work plan two

This is in line with objective two (2) which was mainly based on fresh properties of the combined ternary blend geopolymer mortars determination. The procedures used is presented in Section 3.2.2.

3.2.1.3 Work plan three

This involved the evaluation of the durability performance of ternary-blend alkali activated mortars. The procedures used here is further discussed in Section 3.2.2.

i. Sulphate resistance test

ii. Acid resistance test.

iii. Permeability test (water absorption and sorptivity)

3.2.2 Experimental procedure

The work plans as outlined in Section 3.2.2 was handled with the following procedural stages stated.

3.2.2.1 Material characterization

The material characterizations involved the examination of both the chemical and physical properties of the constituent materials. The physical analysis carried out on the RHA, CPA, MK were Particle size distribution analysis (PSD), specific gravity and moisture content. The chemical analysis conducted on RHA, CPA and MK samples was achieved at the Rolab Research and Diagonistic Laboratory, Ibadan. Which involved packaging about 100g of the powder cementitious materials (PC and SHA) in sealed small polythene bags and sent to the laboratory for Xray Fluorescent (XRF) analysis for determination of oxide composition in accordance to ASTM C618 (2015) using XRF analyzer connected to a computer system for data acquisition.

The physical properties of all the constituent materials was carried out in the Building laboratory of Federal University of Technology, Minna. The properties examined are the particle size distribution (PSD) by sieve method for fine aggregate and the tests to be conducted on cement, RHA, CPA and MK are consistency, setting time and soundness test.

3.2.2.2 Mix proportioning and specimen production

Currently, no standard mix design is available for the production of GPM. This means that the mix design for the production of geopolymer mortar was based on trial and

error with a guide from previous research work in literature. A confirmation of the mix design was done using the outcome of the trial mix test. RHA, CPA, and MK suitable mix design and proper mixing procedure were built up after several trial mixes have been conducted.

3.2.3 Detail method of mortar mix

This research investigated the varying composition of solid binder as independent variable on the durability properties of ternary blend GPM. A trial mix was conducted prior to the casting of experimental specimens. The control variable of this research was the specimens incorporated portland cement only (PCM) and the other mixes were those with variation in binder composite, total five mortar samples were cast with increasing CPA content of 10 %, 30 %, 50 %, 70 % and 90 %. While the remaining contents was two-third of MK and one-third of RHA as shown in Table 3.1.

The methodology of ternary blended approach (mixing three SCMs together) to improve the performance of mortar involves having materials blended together in a ternary mortar mixed in a combination proportion showing in table 3.1. A Binder of 140g was used in preparing the flowability and 300g of binder was used in carrying out the setting time. The Alkaline to binder ratio used was range from 0.7 and the ratio of NaOH to Na_2SiO_3 was 1:2.5 in preparing the mix.

Table 3.1: Mix proportion of Alkali Activator Mortar for optimum CPA content

Mix ID	CPA (%)	MK (%)	RHA (%)	W/B ratio	FA	Na_2SiO_3	NaOH
C90M07S03*	90	7	3	0.35	2.5	0.25	0.1
C70M20S10**	70	20	10	0.35	2.5	0.25	0.1
C50M33S17***	50	33	17	0.35	2.5	0.25	0.1
C30M47S23ββ	30	47	23	0.35	2.5	0.25	0.1
C10M60S30β	10	60	30	0.35	2.5	0.25	0.1

C90M07S03* is geopolymer (containing 90%CPA, 7%MK & 3% RHA), Water to binder (W/B)
C70M20S10** is geopolymer (containing 70%CPA, 20%MK & 10% RHA)
C50M33S17*** is geopolymer (containing 50%CPA, 33%MK & 17% RHA)
C30M47S23ββ is geopolymer (containing 30%CPA, 47%MK & 23% RHA)
C10M60S30β is geopolymer (containing 10%CPA, 60%MK & 30% RHA)

Commented [D47]:

3.2.4 Specimen testing and data collation

The following durability tests were conducted and tested for the purpose of this research work. The tests as thus discussed therein:

Commented [D48]:

3.2.4.1 Compressive test

The compressive strength of specimens will be tested by compressive test in accordance with BS EN 12390-3 (2009) at 7, 28, 56 and 90 days. It is performed under the loading rate of 45kN per minute on the 50 mm cube specimen until the failure occurred. The compressive strength values were obtained by the average of three specimens while the specimen is ensured to be centered and the seat platen is free to move. The test was then run and the maximum force loaded on the specimen recorded.

Commented [D49]:

Commented [D50]:

3.2.4.2 Acid resistance test

The resistance of the geopolymer mortar to acid attack was studied by immersion of cube specimens (50 x 50 mm) in 5% solutions of sulfuric acid with pH of 0.8. The choice of acid

Commented [D51]:

solution and its concentrations was based on practical utilization of concrete as a construction material in sewage pipes, mining, and food processing industries. The testing media was replaced monthly with fresh solutions. The compressive strength of specimen (50 x 50 mm) was measured at 28, 56 and 90 days of exposure.

The assessment of the geopolymer specimens in acidic environment was carried out based on the performance from visual assessment, weight loss and strength loss factor.

Physical assessment

Visual assessment was done and the physical durability effect of the specimen in sulphuric acid (H_2SO_4) solution was critically observed. The assessment was based on the condition of the edges, surface texture, colour, size and shape of the specimen.

Commented [D52]:

Mass loss

The initial mass of the specimens and the weight over an immersion was measured at the respective curing ages (28, 56 & 90 hydration periods) for the determination of mass loss. Thus, due to the deterioration of the specimen by acid, the average values of three specimens was considered for assessment.

Commented [D53]:

Commented [D54]:

Strength loss factor

Strength loss factor is a numerical way of expressing the performance of concrete in state of qualitative means. The deterioration of concrete specimens was investigated at 28, 56 & 90 curing ages by measuring the strength loss factor expressed in percentage and was calculated using the following Equation:

$$SLF = F_{cw} - F_{ca} / F_{cw} * 100\% \quad (3.1)$$

Where: SLF = Strength loss factor after immersion in acid solution

Fcw = Average strength of companion specimen cured in water

Fca = Average strength of the specimen after immersion in acid solution

3.2.4.3 Sulphate resistance test

This test was performed to assess the physical characteristics and response of mortar to attack by immersing the geopolymer mortar specimen in sulphate solution. Sulphate ions in the solution was combined with calcium hydroxide and gypsum to form an expansive reaction. Concrete cubes of 50 mm size were produced and tested for sulphate action. The assessment was made in terms of mass change, visual observation and strength deterioration factor.

Visual assessment

Visual assessment was done to critically observe the physical durability effect of the specimens in Na_2SO_4 solution. The assessment was based on condition of the edges, surface texture, colour, size and shape of the specimen.

Mass change

Deterioration of the geopolymer mortar mixtures immersed in 5% sodium sulphate solution was carried out by measuring change in mass of the specimens after the respective curing ages. The initial weight of the specimens and the weight after the immersion was measured for determination of mass loss due to the deterioration of the specimen by sulphate. The average values of three specimens was considered for assessment.

Strength loss factor (SLF)

The deterioration of concrete specimens was investigated by evaluating the strength distortion factor expressed in percentage, The SLF was measured at their respective ages of immersion and was calculated using Equation (3.2).

$$SLF = Fcw - Fcs\ Fcw * 100\% \quad (3.2)$$

Where: SLF = Strength loss factor after immersion in Sulphate solution

Fcw = The average compressive strength of companion specimen cured in water

Fcs = The average compressive strength of the specimen after immersion in Sulphate solution

3.2.4.6 Water absorption test

The test was conducted in conformity with ASTM C642/C642M (2013), which specifies a method for the determination of water absorption of mortar and concrete specimens. An average of three 50 mm cube specimens was prepared. The cubes were oven dried at temperature of 110 ± 5ºC for 24 hours. The oven dried specimens were allowed to cool in an airtight desiccator of temperature 24 ± 2ºC. At the end of drying and cooling, the specimens were weighed and immersed in water tank at approximately 21 ºC for 48 hours. After removal from water, the specimens were wiped with a dried towel to remove the surface water and weighed. The measured absorption of each test specimen was then calculated as the increase in the weight resulting from the immersion expressed as a percentage of the mass of the dry specimen as shown in the following equation:

$$Wa = (Ms - Md/Md) * 100\% \quad (3.11)$$

Where: Wa = Water absorption (mass %)

Ms = Saturated surface dry mass of the specimen in air

Md = Oven-dry mass of the specimen in air

CHAPTER FOUR

4.0 RESULTS AND DISCUSSION

4.1 Materials Characterization

4.1.1 Particle size distribution (PSD) of fine aggregates

Figure 4.1 presents the particle size distribution of the fine aggregate examined in this study and the summary of the physical properties of the aggregate are highlighted in Table 4.1.

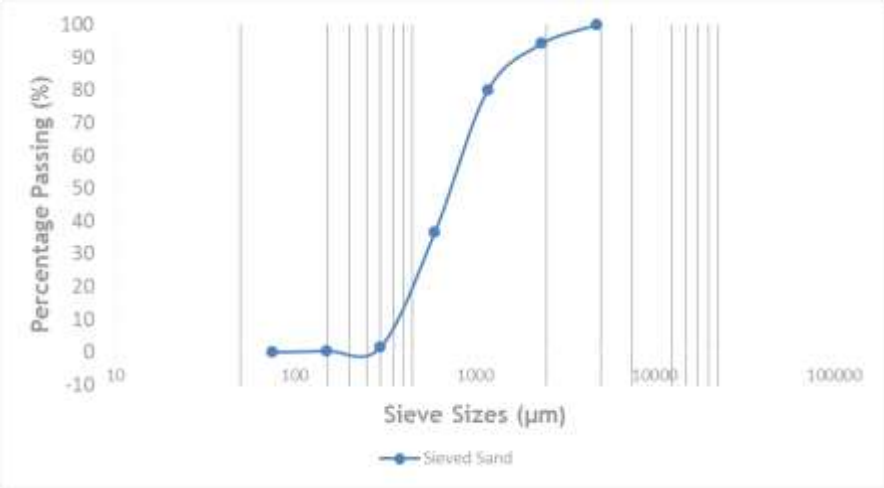

Figure 4.1: Particle size distribution of aggregates

The results revealed that the fine aggregate conformed to the medium sand classification according to Shetty (2004) with uniformity coefficient (C_u) of 2.39, coefficient of curvature (C_c) of 0.94, specific gravity value of 2.82 and fineness modulus (FM) of 2.65. Table 4.1 makes it crystal cleared that the fine aggregate is appropriate for the production of

geopolymer mortar (GPMs) according to the literature (Wilson & Ding, 2007; Rodriguez *et al.*, 2008,. Rostami, 2015).

Commented [D55]:

Table 4.1: Summary of physical properties of the constituent materials

Item	Sand	RHA	CPA	MK	PC
D_{10}	360				
D_{30}	540				
D_{60}	860				
C_u	2.39				
C_c	0.94				
FM	2.65				
SG	2.82	2.8	1.8	2.59	3.15

4.1.2 Chemical analysis of binder

The composition of oxides present in the RHA, CPA and MK were examined in comparism with the CEM II in accordance with the requirements of oxides composition specification for the production of GPM.

4.1.2.1 XRF characterization of binders

The chemical composition and loss on ignition of CEM II as received and RHA, CPA and MK determined by XRF are shown in Table 4.2. The outcome of the test reveals that the RHA, CPA and MK contained majorly SiO_2. Furthermore, it can be seen that the SiO_2 present in them as revealed by the result are 95%, 80.83% and 72.39% with silica-sesquioxide (S-S) ratio (SR) of 166.67, 34.84 and 3.37 with aluminium-sesquioxide ratio (AR) of 3.75, 0.50 and 18.17 respectively which according to ASTM C618 (2015) is affirmed to be a very strong reactive Class F Pozzolan with the sum of silica (95%, 80.83% and 72.39%), alumina (0.45%, 0.77% and 20.35%) and ferric oxides (0.12%, 1.55% and

1.12%) respectively higher than the specified 70%. Also, the CEM II contained 60% CaO which makes it crystal cleared that the PC is majorly calcium oxide and is in conformance with the oxide composition reported in literature (Rostami, 2015; 2021a; Shetty, 2004) for CEM II.

Table 4.2: Oxide Composition of Binder Constituents

Oxides	RHA (%)	CPA (%)	MK (%)	CEM II (%)
SiO_2	95.0	80.83	72.39	25.64
Al_2O_3	0.45	0.77	20.35	5.24
Fe_2O_3	0.12	1.55	1.12	7.15
CaO	0.84	4.24	0.01	60.35
MgO	0.45	-	0.12	0.41
SO_3	0.10	0.83	-	0.11
K_2O	1.50	5.50	3.12	0.05
Na_2O	0.03	0.06	0.34	0.31
M_2O_5	0.10	1.61	0.10	0.04
P_2O_5	0.72	2.50	0.10	0.03
LOI	0.74	2.10	2.35	0.67
$SiO_2 + Al_2O_3 + Fe_2O_3$	95.57	83.15	93.86	12.68
SR	166.67	34.84	3.37	2.07
AR	3.75	0.50	18.17	0.73
Total	100	100	100	100

4.2 Fresh Properties

The setting time and the workability of the readily mix mortar used in GPMs production were explored to know the flow of the slump and the effect of the SCMs utilized on the setting time in comparism with the cement.

4.2.1 Slump flow test

Commented [D56]:

Flow table test was used to observed the spreading of the fresh geopolymer mortar by repeatedly tapping for 25 times on a levelled surface. Throughout the experiment, the rapid setting of ternary-based GPM was noticed as shown in the Table 4.3. the fresh mortar began to set within five to twenty minutes (5-20 mins) right after thoroughly mixing process for the C90M7R3 mix followed by C70M20R10, C50M33R17, C30M47R23 and

C10M60R30 with the initial and final setting times of twenty and sixty minutes (20-60 mins), twenty-five and sixty-five minutes (25-65 mins), thirty and hundred minutes (30-100 mins), forty-five and one-twenty minutes (45-120 mins) respectively.

It was later discovered that the GPM had a very flash setting in comparism with the reference mortar (CGPM) having it initial and final setting times to be one and half hours and three hours respectively while the results also revealed that at a decrease in the cassava peel ash (CPA) percentage replacements then the setting time increases.

Commented [D57]:

Commented [D58]:

Furthermore, the result also showed a descending trend in the spreading width as observed with a decrease in the replacement levels of CPA. Higher CPA content exhibits higher workability and faster settings of the GPM. Hence, it was discovered that the RHA incorporation contributed to the reduction in the spreading width as a result of its hygroscopic nature and thereby accelerate the geopolymerization of the specimens (Gao *et al*., 2016). Lower spreading width achieved by increasing the replacement level of MK-RHA attributed to the content of CaO and thus accelerate the geopolymerization as its rapid reaction with alkali activator (Khan *et al*., 2016).

The initial flow table result for C90M7R3 was 220 mm as shown in plate 1 and table 4. However, the spreading width of the subsequent mixes were found to be slightly reducing from 220 mm to 210 mm, 200 mm, 190 mm, 150 mm and 140 mm for C70M20R10, C50M33R17, C30M47R23 and C10M60R30 respectively. This can be explained by rapid dissolution of CaO as reacted with the activator and on the other hand, the inclusion of the RHA prolong the setting times due to the slow rate of decomposition in RHA particles at ambient temperature (Wang *et al.*,2015).

Table 4.3: Fresh Properties of ternary blended GPMs

Variables	Spreading Width (mm)	Setting time (min)	
		Initial	Final
PCM	220	90	180
C90M7R3	210	5	20
C70M20R10	200	20	60
C50M33R17	190	25	65
C30M47R23	150	30	100
C10M60R30	140	45	120

4.3 Hardened Properties of the GPMs

The influence of aggressive environments in terms of sulphate and acid attack in respect to its visual appearance, mass loss and the strength loss factor (SLF) of the GPMs, and as well as the water absorption of the GPMs were discussed herein.

4.3.1 Influence of sulphate attack on the compressive strength of GPMs

The visual assessment, the mass loss and the compressive strength were monitored in order to understand the primary degradation mechanism.

4.3.1.1 Visual assessment

Plate I showed the view of the GPMs after curing by immersion in 5% sodium sulphate (Na_2SO_4) solution. The colour of the mortar provides extensive and general guide on the effect of sulphate on specimen, whether the colour represents the original surface or not.


28days
56 days
90days
CONTROL
C10M60R30
C30M47R23
C50M33R17
C70M20R10
50/50
50/50
50/50
70/30
70/30
70/30

C90M07R10 

Plate I: Visual appearance of specimen after immersion in Na_2SO_2

Table 4.4 presents the overall visual observation of the specimens after 28, 56 and 90 days of immersion to 5% Na_2SO_4 solution. The assessment was done in terms of the specimen's colour, surface texture, edges and sizes.

Table 4.4a: Physical characteristics of ternary blended GPMs exposed to sulphate solution

Specimen	Physical characteristics of ternary GPMs after 28 days immersion in 5% Na_2SO_4				
	Surface texture	Size	Colour	Edge	Shape
PCM	Slightly deteriorated	No change	Whitish deposit	Perfect	Perfect cube
C90M7R3	Smooth	No change	Little Dark	Perfect	Perfect cube
C70M20R10	Smooth	No change	Little Dark	Perfect	Perfect cube
C50M33R17	Smooth	No change	Little Dark	Perfect	Perfect cube
C30M47R23	Smooth	No change	Little Dark	Perfect	Perfect cube
C10M60R30	Slightly deteriorated	No change	Little Dark	Fine cracks	Perfect cube
Specimen	Physical characteristics of HPC after 56 days immersion in 5% Na_2SO_4				
	Surface texture	Size	Colour	Edge	Shape
PCM	Slightly deteriorated	No change	Whitish deposit	Perfect	Perfect cube
C90M7R3	Smooth	No change	Little Dark	Perfect	Perfect cube
C70M20R10	Smooth	No change	Little Dark	Perfect	Perfect cube
C50M33R17	Smooth	No change	Little Dark	Perfect	Perfect cube
C30M47R23	Smooth	No change	Little Dark	Perfect	Perfect cube
C10M60R30	Slightly deteriorated	No change	Little Dark	Fine cracks	Perfect cube
Specimen	Physical characteristics of HPC after 90 days immersion in 5% Na_2SO_4				

Table 4.4b: Physical characteristics of ternary blended GPMs exposed to sulphate solution

	Surface texture	Size	Colour	Edge	Shape
PCM	Slightly deteriorated	No change	Whitish deposit	Perfect	Perfect cube
C90M7R3	Smooth	No change	Little Dark	Perfect	Perfect cube
C70M20R10	Smooth	No change	Little Dark	Perfect	Perfect cube
C50M33R17	Smooth	No change	Little Dark	Perfect	Perfect cube
C30M47R23	Smooth	No change	Little Dark	Perfect	Perfect cube
C10M60R30	Slightly deteriorated	No change	Little Dark	Fine cracks	Perfect cube

The GPMs appeared to be little dark in colour after hardened and before the immersion on the Na_2SO_4 solution and which as a result, there was no sign of discoloration, expansion and or cracking on the surface of the GPM samples after the immersion at all ages except the mix incorporated 10% CPA, 60% MK and 30% RHA (C10M60R30) covered with net of cracks. In terms of the edges and sizes, it was discovered that there was no deterioration for all the GPMs mixes at all ages. In contrast, PCM samples showed a very minute degree of deterioration and its surface exposed in Na_2SO_4 were coated with a layer of white precipitate which has been confirmed as the Na_2SO_4 hydrates. On the other hand, edges of the PCM samples became rounded and leaching took place due to loss of degraded material. Although, these PCM samples showed no visible expansion and the initial shape was maintained at all the hydration periods.

4.3.1.2 Mass loss

The results of mass loss versus the curing media and ages (i.e.,28, 56 and 90 days) are illustrated in Figure 4.2. It can be observed that the entire specimens exhibited similar behaviour of varied mass losses of the specimens. This was due to non-absorbing of the sulphate particles after 28-, 56- and 90-days immersion. At the end of immersion periods, it

was noticed that the reference mortar (PCM) had the highest mass loss of 29.60%, 32.2% and 32.4% at 28, 56 and 90 days respectively. However, addition of the activators and the SCMs and the removal of the PC to the mixtures significantly control the mass loss of the mortar. From the results presented in Figure 4.2, it can be deduced that the introduction of these materials that led to the GPM productions contributed to the reduction in mass loss in comparism with the PCM and the mass loss increased as the curing ages increases irrespective of the mix. The mass loss of GPMs with 90% CPA, 7% MK and 3% RHA (C90M7R3) gave percentage mass loss values of 28.90%, 31.7% and 32.10% at 28-, 56- and 90-days and 22.40%, 23.6% and 25.59% for the GPM incorporated 70% CPA, 20% MK and 10% RHA (C70M20R10). Also, 14.20%, 16.70% and 17.30% for GPM with 50% CPA, 33% MK and 17% RHA (C50M33R17), 19.10%, 22.30% and 22.90% for GPM with 30% CPA, 47% MK and 23% RHA (C70M47R23) and as well as the GPM incorporated 10% CPA, 60% MK and 30% RHA (C10M60R30) with mass loss of 29.0%, 30.30% and 33.30% at 28, 56 and 90 days respectively. It is interesting to note that the GPMs positively contributed to resistance of Na_2SO_4 attack when compared to that reference mixture (PCM). Application of the RHA in GPM is advantageous under sulphate environment due to the discontinuous pore structure of the ash mortar and amount of calcium hydroxide present in the mortar.

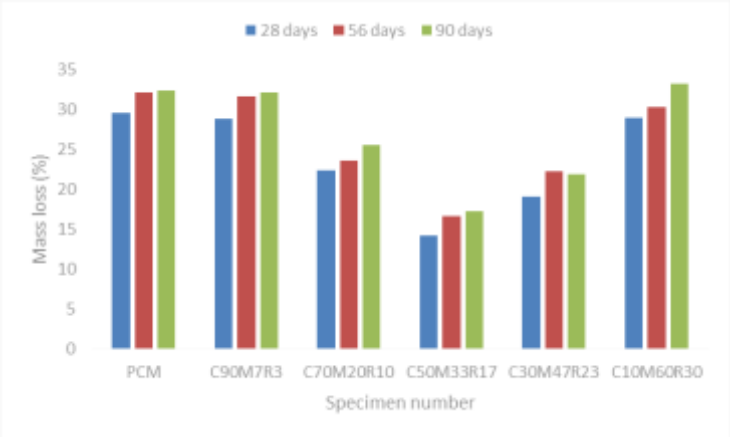

Figure 4.2: Mass loss of ternary blended GPMs subjected to Na_2SO_4 attack

4.3.1.3 Strength loss

Comparisons between GPMs strength cured in both the ambient and Na_2SO_4 media at various ages (28, 56 and 90 days) are shown in Figure 4.3. At the end of 90 days curing age, the strength of mortar specimens immersed in Na_2SO_4 solution is compared with those cured in normal ambient temperature. The difference in the compressive strength between the GPMs cured using ambient temperature and the those immersed in Na_2SO_4 solution is regarded as the strength loss. From the results displayed in the Figure 4.3, it is obvious that the entire specimen suffered strength losses but the loss of some mixes were not drastically detrimental. The strength loss was observed to be more in reference mortar (PCM) specimens when compared to GPMs (C90M7R3, C70M20R10, C50M33R17, C30M47R23 and C10M60R30). The C50M33R17 of the GPM mixes exhibited the lowest loss in strength with the highest residual strength of 98.28%, 94.79% and 89.54% at 28, 56 and 90 days respectively followed by C30M47R23 having residual strengths of 89.15%, 87.49%

and 85.37%, C70M20R10 with residual strengths of 87.18%, 86.06% and 85.20% and as well as 84.92%, 83.54% and 78.46% for the GPM mix C10M60R30 and 73.49%, 72.30% and 71.73% for the GPM mix C90M7R3 at 28, 56 and 90 days respectively. The strength losses values of 6.83 N/mm^2, 9.31 N/mm^2 and 10.19 N/mm^2 were observed for PCM mix at 28, 56 and 90 days respectively. Whereas, the strength loss values of 6.51 N/mm^2, 7.32 N/mm^2 and 8.16 N/mm^2 were recorded in C90M7R3, 3.25 N/mm^2, 4.19 N/mm^2 and 5.16 N/mm^2 for C70M20R10, 2.94 N/mm^2, 4.16 N/mm^2 and 5.40 N/mm^2 for C30M47R23 , 4.05 N/mm^2, 5.08 N/mm^2 and 7.10 N/mm^2 for C10M60R30 and as well as the GPM mix C50M33R17 having the lowest strength loss values of 0.67 N/mm^2, 2.20 N/mm^2 and 4.67 N/mm^2 with the highest residual strength as said earlier at 28, 56 and 90 days respectively. However, the result also revealed that irrespective of the mix, the loss in strength of both the PCM and GPMs kept increasing at an increase in the hydration periods while the loss is more pronounced in PCM in comparism with the GPMs.

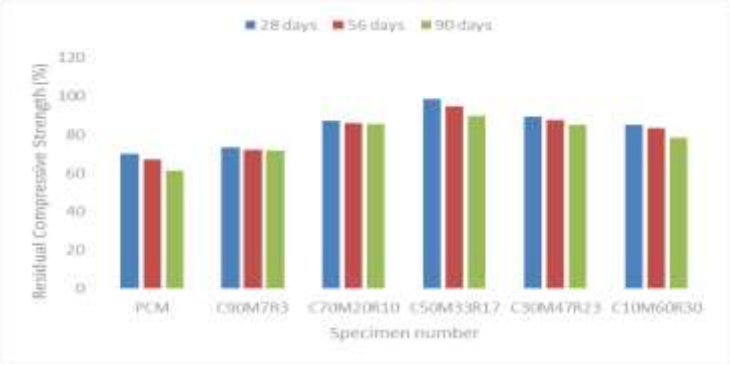

Figure 4.3: Strength losses as caused by Na_2SO_4 attack on ternary blended GPMs

4.3.1.4 Strength loss factor (SLF)

The compressive strength deterioration of the PCM, C90M7R3, C70M20R10, C50M33R17, C30M47R23 and C10M60R30 mortar mixtures due to Na_2SO_4 attack was further expressed in the form of strength loss factor (SLF). Figure 4.4 reveals the SLF after 28-, 56- and 90-days immersion in Na_2SO_4 solution. It can be seen that all of the mixes were affected by the sulphate action and generally developed SLF. The values were found to be higher in PCM with 30.15%, 32.98% and 38.53% SLFs at 28, 56 and 90 days respectively. This is followed by the C90M7R3 with 26.51%, 27.70% and 28.27% and then C10M60R30 with 15.08%, 16.46% and 21.54% SLFs and as well as C70M20R10 with SLFs values of 12.82%, 13.94% and 14.63% at 28, 56 and 90 days respectively. Also, the GPM mix C30M47R23 had the second lowest values of 10.85%, 12.51% and 14.80% at 28, 56 and 90 days respectively and the lowest SLFs were observed in C50M33R17 with 1.71%, 5.21% and 10.46% SLFs at 28, 56 and 90 days respectively. The reason of SLF feature in the test specimens is similar to those earlier stated in strength loss.

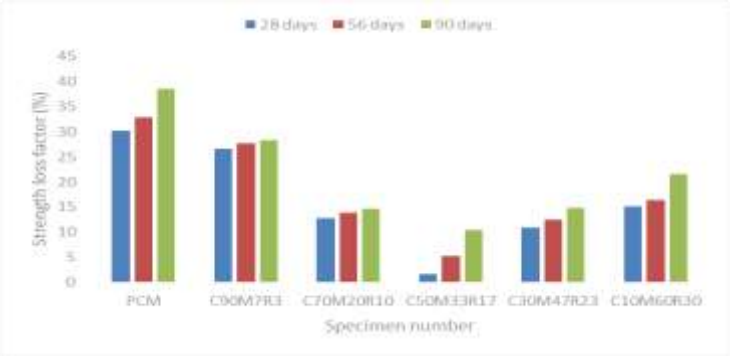

Figure 4.4: Strength loss factor (SLF) of ternary blended GPMs exposed to sulphate solution

4.3.2 Influence of sulphuric acid attack on the compressive strength of GPMs

The visual assessment, the mass loss and the compressive strength were monitored in order to understand the primary degradation mechanism.

4.3.2.1 Visual assessment

Presented in Plate 2 is the visual appearance of the GPMs after curing by immersion in 5% sulphuric acid (H_2SO_4) solution. The colour of the mortar gives a general guide on the impact of the sulphuric acid on the samples, whether the colour represents the original surface or resulting from sulphate attack. Table 4.4 presents the overall visual observation of the specimens after 28, 56 and 90 days of immersion to 5% H_2SO_4 solution. The assessment was also carried out in respect to the specimen's colour, surface texture, edges and size as explained earlier under the influence of sulphate attack.

CONTROL

C10M60R30

C30M47R23

C50M33R23

C70M20R10

C90M07R10

Plate II: Visual appearance of specimen after immersion in H_2SO_4

In general, all samples exposed to H_2SO_4 solutions deteriorated slightly and was particularly visible with the PCM where part of the binder was removed from the surface layer and sand particles became exposed but no sand particles were detached from the GPM binder matrix.

Table 4.5: Physical characteristics of ternary blended GPMs exposed to sulphuric acid solution

Specimen	Physical characteristics of ternary GPMs after 28 days immersion in 5% H_2SO_4				
	Surface texture	Size	Colour	Edge	Shape
PCM	Slightly deteriorated	No change	Whitish deposit	Rounded	Perfect cube
C90M7R3	Smooth	No change	Little Dark	Perfect	Perfect cube
C70M20R10	Smooth	No change	Little Dark	Perfect	Perfect cube
C50M33R17	Smooth	No change	Little Dark	Perfect	Perfect cube
C30M47R23	Smooth	No change	Little Dark	Perfect	Perfect cube
C10M60R30	Slightly deteriorated	No change	Little Dark	Fine cracks	Perfect cube
Specimen	Physical characteristics of HPC after 56 days immersion in 5% H_2SO_4				
	Surface texture	Size	Colour	Edge	Shape
PCM	Slightly deteriorated	No change	Whitish deposit	Rounded	Perfect cube
C90M7R3	Smooth	No change	Little Dark	Perfect	Perfect cube
C70M20R10	Smooth	No change	Little Dark	Perfect	Perfect cube
C50M33R17	Smooth	No change	Little Dark	Perfect	Perfect cube
C30M47R23	Smooth	No change	Little Dark	Perfect	Perfect cube
C10M60R30	Slightly deteriorated	No change	Little Dark	Fine cracks	Perfect cube
Specimen	Physical characteristics of HPC after 90 days immersion in 5% H_2SO_4				
	Surface texture	Size	Colour	Edge	Shape
PCM	Slightly deteriorated	No change	Whitish deposit	Rounded	Perfect cube
C90M7R3	Smooth	No change	Little Dark	Perfect	Perfect cube
C70M20R10	Smooth	No change	Little Dark	Perfect	Perfect cube
C50M33R17	Smooth	No change	Little Dark	Perfect	Perfect cube
C30M47R23	Smooth	No change	Little Dark	Perfect	Perfect cube
C10M60R30	Slightly deteriorated	No change	Little Dark	Fine cracks	Perfect cube

On the other hand, edges of the PCM samples became rounded and leaching took place due to loss of degraded material. Although, these PCM samples showed no visible expansion and the initial shape was maintained at all the hydration periods.

The GPMs appeared to be little dark in colour after hardened and before the actual exposure to the H_2SO_4 solution there was a sign of little discoloration without any expansion and or cracking on the surface of the GPM samples after the immersion at all ages except the mix incorporated 10% CPA, 60% MK and 30% RHA (C10M60R30) having minute cracks. In terms of the edges and sizes, it was discovered that there was no deterioration for all the GPMs mixes at all ages. In contrast, PCM samples showed a very minute degree of deterioration and its surface exposed in H_2SO_4 were coated with little layer of white precipitate which has been confirmed as the H_2SO_4 hydrates.

4.3.2.2 Mass loss

The mass changes in mortar samples during the period of immersion in H_2SO_4 solutions is shown in Figure 4.5. The rate of mass loss in both the PCM and GPMs sample exposed to H_2SO_4 solutions was increasing from one cycle to the next during the hydration periods but the loss was highly pronounced in PCM with 31.25%, 33.30% and 34.10% at 28, 56 and 90 days respectively compare to the GPMs. The results also revealed that the sample C90M7R3 reached maximum mass loss of 29.50%, 32.55% and 32.95% at 28, 56 and 90 days respectively when exposed to H_2SO_4 solutions with 5% by weight of curing water concentrations. The same trend were followed in other GPM mixes with an increase in the mass loss as the hydration periods increases and with the GPM samples C70M20R10 having the values of 24.20%, 23.99% and 26.45% at 28, 56 and 90 days respectively followed by the GPM mix C50M30R20 having the lowest mass loss of 16.50%, 18.25%

and 19.22% at 28, 56 and 90 days respectively. The GPM mix C30M47R23 had the values of 20.25%, 25.05% and 26.59% and as well as 29.50%, 30.69% and 33.45% for C10M60R30 GPM mix.

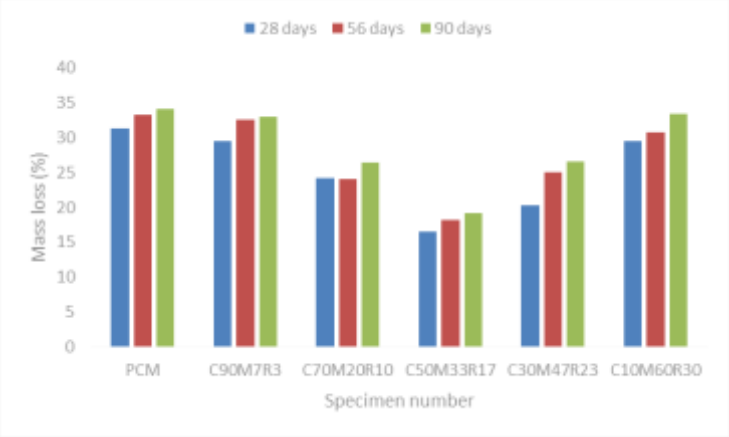

Figure 4.5: Mass loss of ternary blended GPMs subjected to H_2SO_4 attack

In contrast, the PCM mass loss was above the mass loss in all the GPM mixes. As evidenced by the colour change of the sample's surface, the difference was most probably related to the decalcification of hep and formation of a layer sulphate salts, gypsum and ettringite (Peyvandi *et al*., 2015), on the surface of the sample. Most likely, these salts also formed in the pores of the outermost surface layer of the samples. At this stage, no degradation was observed and the mass loss was the result of high degree of hep decalcification and most importantly, the result of progressive degradation of the surface layer caused by pressure exerted by expansive crystals of the salt formed inside the pore structure. This suggest that the degraded layer of the material in GPM mixes acted as a

buffer zone and slowed down further progression of the acid attack, thus providing better overall resistance against the acid attack than the PCM counterparts.

4.3.2.3 Strength loss

Comparisons between GPMs compressive strength cured in both ambient and sulphuric acid (H_2SO_4) media at various hydration periods (28, 56 and 90 days) are shown in Figure 4.6. At the end of 90 days curing age, the strength of mortar specimens immersed in H_2SO_4 solution is compared with those cured in normal ambient temperature. The difference between the GPMs compressive strength cured in ambient temperature and those immersed in H_2SO_4 solution is referred to as the strength loss. From the results showing in Figure 4.6, it is crystal cleared that the whole specimens suffered strength losses and the loss of some mixes were not drastically detrimental. The strength loss was observed to be more in reference mortar (PCM) as discussed under the sulphate attack when compared to GPMs (C90M7R3, C70M20R10, C50M33R17, C30M47R23 and C10M60R30). The C50M33R17 of the GPM mixes exhibited the lowest loss in strength with the highest residual strength of 94%, 90% and 85% at 28, 56 and 90 days respectively followed by C30M47R23 having residual strengths of 84%, 82% and 81%, C70M20R10 with residual strengths of 82%, 81% and 81% and as well as 80%, 77% and 74% for the GPM mix C10M60R30 and 70%, 61% and 58% for the GPM mix C90M7R3 at 28, 56 and 90 days respectively. The strength losses values of 8.40 N/mm^2, 11.31 N/mm^2 and 12.19 N/mm^2 were observed for PCM mix at 28, 56 and 90 days respectively. Whereas, the strength loss values of 8.51 N/mm^2, 9.30 N/mm^2 and 10.16 N/mm^2 were recorded in C90M7R3, 5.25 N/mm^2, 6.19 N/mm^2 and 7.16 N/mm^2 for C70M20R10, 4.94 N/mm^2, 6.16 N/mm^2 and 7.40 N/mm^2 for C30M47R23 , 6.05 N/mm^2, 7.08 N/mm^2 and 9.10 N/mm^2 for C10M60R30 and as well as the GPM mix

C50M33R17 having the lowest strength loss values of 2.67 N/mm^2, 4.20 N/mm^2 and 6.67 N/mm^2 with the highest residual strength as said earlier at 28, 56 and 90 days respectively. However, the result also revealed that irrespective of the mix, the loss in strength for both the PCM and GPMs kept increasing at an increase in the hydration periods while the loss is more pronounced in PCM in comparism with the GPMs.

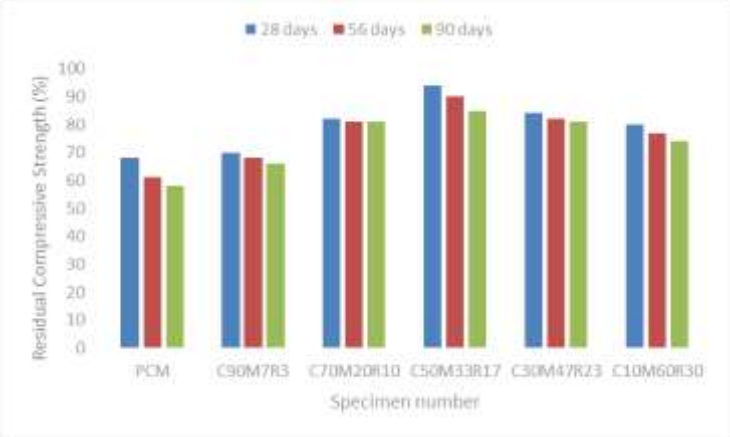

Figure 4.6: Strength losses as caused by H_2SO_4 attack on ternary blended GPMs

4.3.2.4 Strength loss factor (SLF)

The deterioration in the strength of the PCM and GPMs mixtures due to H_2SO_4 attack was further expressed in the form of strength loss factor (SLF). Figure 4.7 presents the SLF of the system after 28-, 56- and 90-days immersion in H_2SO_4 solution. It was discovered that all the mixes were affected by the sulphuric action and thereby led generally to SLF developments. The outcome of the results also followed the same trend with the sulphate action as explained earlier with the values found to be higher in PCM with 32%, 3% and

42% SLFs at 28, 56 and 90 days respectively. This is followed by the C90M7R3 with 30%, 32% and 34% and then C10M60R30 with 20%, 23% and 26% SLFs and as well as C70M20R10 with SLFs values of 18%, 19% and 19%, at 28, 56 and 90 days respectively. Also, the GPM mix C30M47R23 had the second lowest values of 16%, 18% and 119% at 28, 56 and 90 days respectively and the lowest SLFs were observed in C50M33R17 with 6%, 10% and 15% SLFs at 28, 56 and 90 days respectively. The reason of SLF feature in the test specimens is similar to those earlier stated in strength loss. Considerably higher C_3A content in the cement should in theory make it more prone to sulphuric acid attack. The RHA and other SCMs chemically binds the CH in the form of C-S-H making it unavailable for sulphuric, gypsum and ettringite, thus reducing the specimen permeability, thereby resists sulphate ion penetration in to the concrete (Peyvandi *et al.*, 2015).

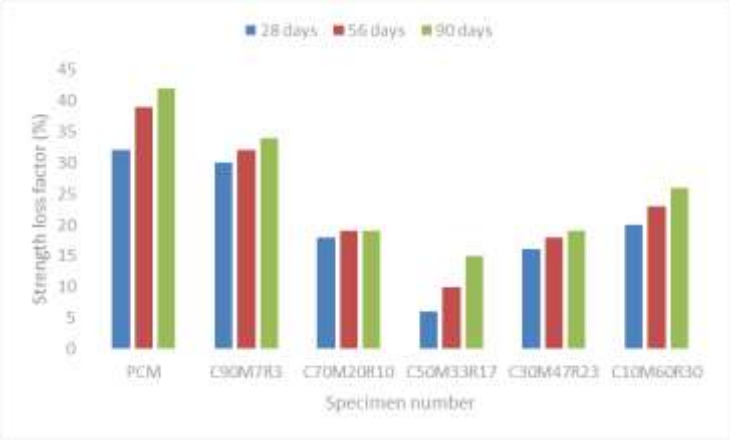

Figure 4.7: Strength loss factor (SLF) of ternary blended GPMs exposed to acid solution

4.3.3 Water absorption of ternary blended GPMs

Figure 4.8 illustrates the water absorption rate of geopolymer samples with different compositions of binders cured at 28, 56 and 90 days. The overall variance of 65.10% in water absorption rate within the range of between 10.23% to 16.89% was manipulated by the varying composition of geopolymer binder comprises of CPA, MK and RHA. A decreasing trend of water absorption rate was observed with a decrease in CPA contents up to the GPM mix incorporated 50% CPA, 33% MK and 17% RHA (C50M33R17) which happened to be the lowest absorption and later increased slightly for the GPM s incorporated C30M47R23 and C10M60R30. PCM has the highest absorption rate of 16.89% at 90 days followed by C90M7R3 having 16.35% also at 90 days, yet dropped to 15.95% when 20% of CPA replacement had been removed from the composition of the binders. The absorption was consecutively decreased to 10.25%, 14.07% and 16.14% with further decreasing in replacement of CPA at every 20% interval up to C10M60R30 and with the GPM mix C50M33R17 having the lowest absorption of 10.25% at 90 days. This can be explained by the degree of geopolymerization as well as the resultant product. RHA is relatively low reactivity at ambient temperature curing, yet inclusion of CPA and MK could accelerate the dissolution of the RHA particle (Yusuf *et al*., 2014b). Large amount of unreacted RHA and MK particles were spotted in C10M60R30 as it contained lowest dosage of CPA as shown in Figure 4.

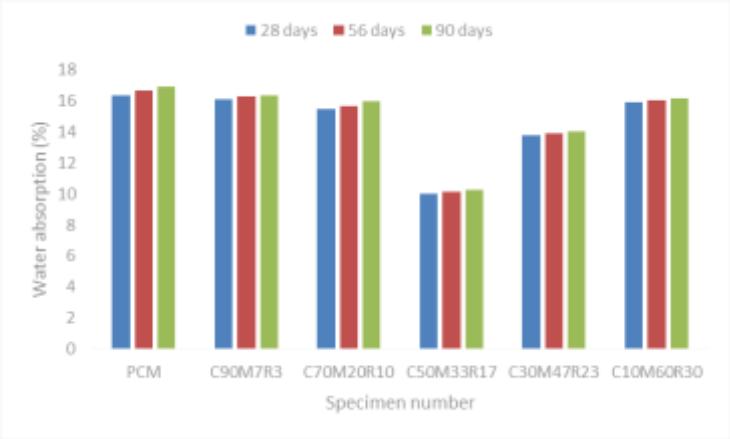

Figure 4.8: Water absorption of ternary blended GPMs

The unreacted particles very often are found in hollow cavities and it tends to create pores in the geopolymer paste (Raybar *et al*., 2014). However, about 60-70% reduction in water absorption for C50M33R17 attributed to 40% increment in CPA replacement. The result also revealed that the GPM is more resistance to moisture penetration in comparism with the reference mortar (PCM) and the absorption increased as the hydration periods increases.

4.4 Summary of Findings

The following are the inferences deduced from the study:

i. The composition of the CPA, MK and RHA's chemical oxide conforms to class F of ASTM-C618 (2015), minimum requirements for pozzolans and can therefore be used as SCMs with the required physiochemical properties.

ii. The visual assessment of GPMs cured in Na_2SO_4 solution as well as H_2SO_4 showed white precipitate crystals only on PCM with minute patterns of crack only on GPM mix C10M60R30 while other GPM mixes showed little dark colour.

iii. All the GPM mixes irrespective of the chemical environment (either Na_2SO_4 or H_2SO_4) used in this study improved the strength of the mortar in comparism with the reference mortar (PCM).

iv. Na_2SO_4 as a curing media as well as H_2SO_4 resulted in to loss in the mass and compressive strength values of both the PCM and GPMs and the loss is more pronounced in PCM while the H_2SO_4 yielded the highest loss. The trend however increased as the hydration periods increased.

v. The ternary GPMs absorption rate examined resulted to an increment as the hydration periods increases and the absorption is more pronounced with samples in H_2SO_4 curing media while the PCM yielded the highest for both when compared.

vi. C50M33R17 (i.e., GPM incorporated 50% CPA, 33% MK and 17% RHA) performed best in resisting both the Na_2SO_4 and H_2SO_4 attack by exhibiting the highest residual strength implying better resistance to chemical attack.

CHAPTER FIVE

5.0 CONCLUSION AND RECOMMENDATIONS

5.1 Conclusion

The study explored the development of alkali-activated RHA-CPA-MK ternary blended geopolymer mortar (GPM) using sodium silicate (Na_2Si_3) and sodium hydroxide (NAOH) solution with 9M constant concentration as alkaline activators under both the aggressive and ambient-temperature curing media. The results revealed that the setting time prolonged as the replacement levels of RHA-MK increased at a decrease in replacement levels of CPA. The GPM discovered to be more resistance to water absorption as compared to PCM while it was observed that the absorption increases as the hydration periods increases.

Furthermore, both the PCM and GPM samples studied suffered mass and strength losses in both the acid and sulphate solution and the loss increases at an increase in the hydration periods while the loss as caused by sulphuric acid is more pronounced. The losses were observed to be higher in PCM as compared to the GPMs while the mix incorporated 50% CPA, 33% MK and 17% RHA (C50M33R17) was observed to be better compared to other mixes in durability performance.

5.2 Recommendations

The study hereby recommends the following:

i. Ternary blended of CPA, MK and RHA with the composition (C50M33R17) should be adopted as the SCMs for 9M concentrations of alkali activators for good durability performance in aggressive sulphate and sulphuric acid environment.

Commented [D59]:

Commented [D60]:

5.3 Contribution to Knowledge

A thoroughly explanation and better insight on the rate of hardening and strength development of ternary blended geopolymer among RHA, CPA and MK with ambient and aggressive chemicals curing is provided in this research. Therefore, the optimum synthesis of RHA, CPA and MK ternary blended geopolymer binder is obtained in this research and the outcome of the optimum synthesized can be applied to either mortar or concrete product. Also, the environmental issue associated with Portland cement production is minimized through this research. Maximizing the utilization of waste products by proving and promoting the waste materials such as RHA, CPA and MK are of great benefit to building structures in terms of strength and exposure to acid or sulphate attack as well as eco-friendly technology.

Instead of disposing the RHA and CPA in landfill or ash ponds, utilizing them in binary or ternary blended geopolymer as better alternative to Portland cement mortar/concrete will create a reduction in wastage and pollution. Furthermore, geopolymer contributes to carbon footprint lowering and approximately 9% lower in CO_2-e compare to Portland Cement mortar/concrete after taking account of treatment, mining, transportation and alkali activators for geopolymer (Turner & Collins, 2013). Therefore, geopolymer has great potential in reducing pollution, climate-changing impact and greenhouse effect.

Sulphate and acid attack on mortar/concrete structures in particular for waste water transport and treatment infrastructure and agricultural applications as well as for a repair. The currently used measure to minimize or reduce such deterioration are costly and, in many cases, required periodic renewal. This work has allowed greater understanding of the performance of a commercial geopolymer binder system in harsh sulphate and acidic

environments and will assist in the design of alternative concrete/mortar. By using these more resistant geopolymer materials, maintenance cost will be reduced and service life increased.

5.4 Areas for further Studies

i. The effect of the sulphate and the sulphuric acid should be further explored at a period beyond what is being studied in this report.
ii. Other aggressive chemical environments should be studied using the same materials.
iii. The effect should be investigated on both the strength and durability properties of GPMs.

REFERENCES

ACI Committee (2001). Guide to durable concrete. American Concrete Institute.

Adesanya, O. A., Oluyemi, K. A., Josiah, S. J., Adesanya, R., Shittu, L., Ofusori, D. & Babalola, G. (2008). Ethanol production by Saccharomyces cerevisiae from cassava peel hydrolysate. *The Internet Journal of Microbiology*, 5(1), 25-35.

Alanazi, H., Yang, M., Zhang, D., & Gao, Z. J. (2016). Bond strength of PCC pavement repairs using metakaolin-based geopolymer mortar. *Cement and Concrete Composites*, 65, 75-82.

Allahverdi, A. & Skvara, F. (2006). Sulfuric acid attack on hardened paste of geopolymer cements-part 2. Corrosion mechanism at mild and relatively low concentrations. Ceramics Silikaty, 50(1), 1-9.

Aliabdo, A. A., Abd Elmoaty, A. E. M. & Salem, H. A. (2016). Effect of water addition, plasticizer and alkaline solution constitution on fly ash based geopolymer concrete performance", *Construction and Building Materials*, , 121, . 694–703.

Allahverdi, A. & Skvara, F. (2005). Sulfuric acid attack on hardened paste of geopolymer cements-Part 1 Mechanism of corrosion at relatively high concentrations, *journal Ceramics-Silikáty*, 49, 225-238.

Aliques-Granero, J., Tognonvi, T. M . & Tagnit-Hamou, A. (2017). Durability test methods and their application to AAMs: case of sulfuric-acid resistance. Materials and structures, 50(1), 1–14.

Al-Majidi, M. H., Lampropoulos, A., Cundy, A. & Meikle, S. (2016) „Development of geopolymer mortar under ambient temperature for in situ alications", *Construction and* Building Materials, 120, 198–211.

Altwair, N. M. & Kabir, S. (2010). Green concrete structures by replacing cement with pozzolanic materials to reduce greenhouse gas emissions for sustainable environment. In 6th International Engineering and Construction Conference, Cairo, Egypt, 269-279.

Arbi, K., Nedeljkovic, M., Zuo, Y. & Ye, G. (2016). A review on the durability of alkali-activated fly ash/slag systems: advances, issues, and perspectives. Industrial & Engineering Chemistry Research, 55(19), 5439-5453.

ASTM C 1012 (2019). Standard Specification for Concrete Aggregates, ASTM International, West Conshohocken, PA.

ASTM C33/C33M (2019), Standard Specification for Concrete Aggregates, ASTM International, West Conshohocken, PA,

ASTM C642/C642M (2013). Standard Test Method for Density, Absorption, and Voids in Hardened Concrete, ASTM International, West Conshohocken, PA.

ASTM C1585/C1585M (2020), Standard Test Method for Measurement of Rate of Absorption of Water by Hydraulic-Cement Concretes, ASTM International, West Conshohocken, PA

ASTM C125/C125M (2015). Standard Terminology Relating to Concrete and Concrete Aggregates. Annual Book of ASTM Standards, *American Society for Testing and Materials*, Philadelphia, USA.

ASTM C618 (2012) Standard specification for coal fly ash and raw or calcined natural pozzolan for use as a mineral admixture in concrete. *Annual Book of ASTM Standards*, Philadelphia, USA.

Ayangade, J. A., Olusola, K. O., Ikpo, I. J. & Ata, O. (2004). Effect of granite dust on the performance characteristics of kernelrazzo floor finish. Building and Environment, 39, 1207-1212.

Bakharev, T., Sanjayan, J.G. & Chen, Y.B. (2003). Resistance of alkali-activated slag concrete to acid attack. *Cement and Concrete Research*. 33, 1607-1611.

Bakharev, T. (2005). Resistance of geopolymer materials to acid attack, *Cement and Concrete Research*. 35, 658-670.

Balaguru, P. (1998). Geopolymer for protective coating of transportation infrastructures o. Document Number).

Bassuoni, M. T. & Nehdi, M. L. (2007). Resistance of self-consolidating concrete to sulfuric acid attack with consecutive pH reduction. Cement and Concrete Research 37(7), 1070–1084.

Barbhuiya, S., & Kumala, D. (2017). Behaviour of a sustainable concrete in acidic environment. Sustainability, 9(9), 1556.

Bakharev, T., Sanjayan, J. G., & Cheng, Y. B. (2002). Sulfate attack on alkali-activated slag concrete. Cement and Concrete research, 32(2), 211-216.

Bernal, S. A., Rodríguez, E. D., Mejía de Gutiérrez, R., & Provis, J. L. (2012). Performance of alkali-activated slag mortars exposed to acids. Journal of Sustainable Cement-Based Materials, 1(3), 138-151.

Behfarnia, K., & Rostami, M. (2017). An assessment on parameters affecting the carbonation of alkali-activated slag concrete. Journal of Cleaner Production, 157, 1-9.

Behfarnia, K., & Shahbaz, M. (2018). The effect of elevated temperature on the residual tensile strength and physical properties of the alkali-activated slag concrete. Journal of Building Engineering, 20, 442-454.

Bondar, D., Ma, Q., Soutsos, M., Basheer, M., Provis, J. L., & Nanukuttan, S. (2018). Alkali activated slag concretes designed for a desired slump, strength and chloride diffusivity. Construction and Building Materials, 190, 191-199.

Brooks, J. J., & Johari, M. M. (2001). Effect of metakaolin on creep and shrinkage of concrete. *Cement and Concrete Composites*, 23(6), 495-502.

BS EN 197-1 (2011). Cement Part 1: Composition, specifications and conformity criteria for common cements, British Standards Institute.

BS EN 1008 (2015). Mixing Water for Concrete-Specification for Sampling, Testing and Assessing the Suitability of Water, British Standards Institute.

BS EN 12390-3 (2009) Compressive strength, Test specimens, Concretes, Compression testing, Cement and concrete technology, Mechanical testing, Failure (mechanical). British Standard Institute, London, United Kingdom (UK).

Burciaga-Díaz, O., Magallanes-Rivera, R., & Escalante-García, J. (2013). Alkali activated slag-metakaolin pastes: strength, structural, and microstructural characterization. Journal of Sustainable Cement-Based Materials, 2(2), 111-127.

Collepardi, M. (2003). A state-of-the-art review on delayed ettringite attack on concrete. Cement and Concrete Composites, 25(4-5), 401-407.

Collepardi, M. (2001). Ettringite formation and sulfate attack on concrete. ACI Special Publications, 200, 21-38.

Chang, J. (2003). A study on the setting characteristics of sodium silicate-activated slag pastes. Cement and Concrete Research, 33(7), 1005-1011.

Chi, M.-c., Chang, J.-j., & Huang, R. (2012). Strength and drying shrinkage of alkali-activated slag paste and mortar. *Advances in Civil Engineering*.

Cheah, C. B., Chung, K. Y., Ramli, M. & Lim, G. K. (2016). The engineering properties and microstructure development of cement mortar containing high volume of inter-grinded GGBS and PFA cured at ambient temperature, *Construction and Building Materials*, 122, 683–693.

Chengning, W. U. (1993). Properties and applications of alkali-slag cement. Journal of the Chinese Ceramic Society, 21(2), 176–181.

Cho, Y., Park, K., Jung, S., & Chung, Y. (2018). A Study on the Sulfate Resistance of Alkali Activated FA Based Geopolymer and GGBFS Blended Mortar with Various Sulfate Types.

Collins, F. & Sanjayan, J. (2008). Unsaturated capillary flow within alkali activated slag concrete, *Journal of Materials in Civil Engineering*, 20(9), 565–570.

Davidovits, J. (2002). 30 years of successes and failures in geopolymer applications. Market trends and potential breakthroughs. Paper presented at the Keynote Conference on Geopolymer Conference.

Davidovits, J. (1994). High-alkali cements for 21st century concretes. *Special Publication*, 144, 383-398.

Davidovits, J. & Comrie, D. (1988). Long term durability of hazardous toxic and nuclear waste disposals. In Proceedings of Geopolymer, 88 (1).

Deb, P. S., Nath, P. & Sarker, P. K. (2014). The effects of ground granulated blastfurnace slag blending with fly ash and activator content on the workability and strength properties of geopolymer concrete cured at ambient temperature, *Materials and Design*, 62, 32–39.

Deb, P. S., Sarker, P. K., & Barbhuiya, S. (2016). Sorptivity and acid resistance of ambient-cured geopolymer mortars containing nano-silica. Cement and Concrete Composites, 72, 235-245.

De Vargas, A. S., Dal Molin, D. C., Vilela, A. C., Da Silva, F. J., Pavão, B., & Veit, H. (2011). The effects of Na_2O/SiO_2 molar ratio, curing temperature and age on compressive strength, morphology and microstructure of alkaliactivated fly ash-based geopolymers. *Cement and concrete composites*, 33(6), 653-660.

Dimas, D., Giannopoulou, I., & Panias, D. (2009). Polymerization in sodium silicate solutions: a fundamental process in geopolymerization technology. Journal of materials science, 44(14), 3719-3730.

Ding, J. T., & Li, Z. (2002). Effects of metakaolin and silica fume on properties of concrete. *Materials Journal*, 99(4), 393-398.

Duggal, S. K. (2008). *Building Materials*. New Age International Publishers, New Delhi, India. 142-300.

Duxson, P., Provis, J. L., Lukey, G. C., & Van Deventer, J. S. (2007). The role of inorganic polymer technology in the development of 'green concrete'. Cement and Concrete Research, 37(12), 1590-1597.

Dwivedia, V. N., Singhb, N. P., Dasa, S. S., & Singha, N. B. (2006). A new pozzolanic material for cement industry: Bamboo leaf ash. *International Journal of Physical Sciences*, 1(3), 106-111.

Edmeades, R. M., Hewlett, P. C. (2006). *Cement admixtures*. *Lea's Chemistry of Cement and Concrete*. 4th ed., Peter C. Hewlett edt., Elsevier, 843-863.

El-Hachem, R., Rozière, E., Grondin, F., & Loukili, A. (2012). New procedure to investigate external sulphate attack on cementitious materials. Cement and Concrete Composites, 34(3), 357-364.

Gao, X., Yu, Q. L. & Brouwers, H. J. H. (2015). Characterization of alkali activated slag–fly ash blends containing nano-silica, *Construction and Building Materials*, 98, . 397–406.

Gao, X., Yu, Q. L. & Brouwers, H. J. H. (2016). Assessing the porosity and shrinkage of alkali activated slag-fly ash composites designed alying a packing model, *Construction and Building Materials*, 119, 175–184.

Garcia-Lodeiro, I., Palomo, A., Fernández-Jiménez, A., & Macphee, D. (2011). Compatibility studies between NASH and CASH gels. Study in the ternary diagram Na2O–CaO– Al2O3–SiO2–H2O. *Cement and Concrete Research*, 41(9), 923-931.

Geissert, D. G., Li, S., Frantz, G. C., & Stephens, J. E. (1999b). Splitting prism test method to evaluate concrete-to-concrete bond strength. *ACI Materials Journal*, 96, 359-366.

Harrison, W.H. (1987). Durability of concrete in acidic soils and waters, *Concrete*. 1, 18-24.

Hardjito, D., Wallah, S., Sumajouw, D., & Rangan, B. (2005). Introducing fly ashbased geopolymer concrete: manufacture and engineering properties. Paper presented at the 30th Conference on our World in Concrete and Structures, 23-24.

Hardjito, D., & Shaw Shen, F. U. N. G. (2011). Parametric study on the properties of geopolymer mortar incorporating bottom ash. In EACEF-International Conference of Civil Engineering, 1, 562-567.

Heikal, M., Nassar, M. Y., El-Sayed, G., & Ibrahim, S. M. (2014). Physico-chemical, mechanical, microstructure and durability characteristics of alkali activated Egyptian slag. Construction and Building Materials, 69, 60-72.

Hu, S., Wang, H., Zhang, G., & Ding, Q. (2008). Bonding and abrasion resistance of geopolymeric repair material made with steel slag. *Cement and concrete composites*, 30(3), 239-244.

Islam, A., Alengaram, U. J., Jumaat, M. Z. & Bashar, I. I. (2014). The development of compressive strength of ground granulated blast furnace slag-palm oil fuel ash-fly ash based geopolymer mortar, *Materials and Design*, 56, 833–841.

Islam, A., Alengaram, U. J., Jumaat, M. Z., Bashar, I. I. & Kabir, S. M. A. (2015). Engineering properties and carbon footprint of ground granulated blast-furnace slag-palm oil fuel ash-based structural geopolymer concrete, *Construction and Building Materials*, 101, 503–521.

Kazemian, A., Gholizadeh Vayghan, A. & Rajabipour, F. (2015). Quantitative assessment of parameters that affect strength development in alkali activated fly ash binders, *Construction and Building Materials*, 93, 869–876.

Komljenović, M., Baščarević, Z., Marjanović, N., & Nikolić, V. (2013). External sulfate attack on alkali-activated slag. Construction and Building Materials, 49, 31-39.

Komnitsas, K., & Zaharaki, D. (2007). Geopolymerisation: A review and prospects for the minerals industry. Minerals Engineering, 20(14), 1261-1277.

Kong, D. L., Sanjayan, J. G., & Sagoe-Crentsil, K. (2007). Comparative performance of geopolymers made with metakaolin and fly ash after exposure to elevated temperatures. Cement and Concrete Research, 37(12), 1583-1589.

Lim, N. H. A. S., Ismail, M. A., Lee, H. S., Hussin, M. W., Sam, A. R. M., & Samadi, M. (2015). The effects of high volume nano palm oil fuel ash on microstructure properties and hydration temperature of mortar. Construction and Building Materials, 93, 29-34.

Mellado, A., Pérez-Ramos, M. I., Monzó, J., Borrachero, M. V., & Payá, J. (2017). Resistance to acid attack of alkali-activated binders: simple new techniques to measure susceptibility. Construction and Building Materials, 150, 355-366.

Mirza, J., Durand, B., Bhutta, A. R., & Tahir, M. M. (2014). Preferred test methods to select suitable surface repair materials in severe climates. *Construction and Building Materials*, 50, 692-698.

Mohamed, O. A. (2019). A review of durability and strength characteristics of alkali-activated slag concrete. Materials, 12(8), 1198.

Momayez, A., Ehsani, M., Ramezanianpour, A., & Rajaie, H. (2005). Comparison of methods for evaluating bond strength between concrete substrate and repair materials. *Cement and concrete research*, 35(4), 748-757.

Monteiro, P. J., & Kurtis, K. E. (2003). Time to failure for concrete exposed to severe sulfate attack. Cement and Concrete research, 33(7), 987-993.

Monteny, J., Vincke, E., Beeldens, A., De Belie, N., Taerwe, L., Van Gemert, D., & Verstraete, W. (2000). Chemical, microbiological, and in situ test methods for biogenic sulfuric acid corrosion of concrete. Cement and Concrete Research, 30(4), 623-634.

Mostofinejad, D., Nosouhian, F., & Nazari-Monfared, H. (2016). Influence of magnesium sulphate concentration on durability of concrete containing micro-silica, slag and limestone powder using durability index. Construction and Building Materials, 117, 107-120.

Nath, P., & Sarker, P. K. (2015a). Use of OPC to improve setting and early strength properties of low calcium fly ash geopolymer concrete cured at room temperature. *Cement and Concrete Composites*, 55, 205-214.

Nath, P., Sarker, P. K., & Rangan, V. B. (2015b). Early age properties of low calcium fly ash geopolymer concrete suitable for ambient curing. Procedia Engineering, 125, 601-607.

Nath, S. K., Maitra, S., Mukherjee, S. & Kumar, S. (2016). Microstructural and morphological evolution of fly ash based geopolymers, *Construction and Building Materials*, 111-119.

Neville, A. M. (2011). Properties of Concrete. Prentice Hall: Pearson Educational Limited.

NIS 444-1 (2003). Composition, specification and conformity criteria for common cements. Standards Organisation of Nigeria.

Obada, K. N., Haque, N. M., Jamal, M., & Khatib, J. M. (2008). Sustainability and Emerging Concrete Materials and their Relevance to the Middle East. *The Open Construction and Building Technology Journal*, 103-110.

Ogundiran, M. B., & Kumar, S. (2015). Synthesis and characterisation of geopolymer from Nigerian Clay. *Applied Clay Science*, 108, 173-181.

Ojo, G. P., Igbokwe, U. G., Egbuachor, C. J., & Nwozor, K. K. (2017). Geotechnical properties and geochemical composition of kaolin deposits in

parts of Ifon, Southwestern Nigeria. American Journal of Engineering Research (AJER), 6, 15-24.

Olawale, M. D. (2013). Syntheses, characterization and binding strength of geopolymers: A review. International Journal of Materials Science and Applications, 2(6), 185-193.

Olonade, K. A., & Mohammed, H. (2019). Review of selected bio-wastes as potential materials for alkali-activation for cement-based products. *Nigerian Journal of Technological Development*, 16(3), 120-126.

Pacheco-Torgal, F., Castro-Gomes, J., & Jalali, S. (2008a). Adhesion characterization of tungsten mine waste geopolymeric binder. Influence of OPC concrete substrate surface treatment. *Construction and Building Materials*, 22(3), 154-161.

Pacheco-Torgal, F., Castro-Gomes, J., & Jalali, S. (2008b). Alkali-activated binders: a review. Part 2. About materials and binders manufacture. *Construction and Building Materials*, 22(7), 1315-1322.

Pacheco-Torgal, F., Labrincha, J., Leonelli, C., Palomo, A., & Chindaprasit, P. (2014). Handbook of alkali-activated cements, mortars and concretes: Elsevier.

Palomo, A., Blanco-Varela, M. T., Granizo, M., Puertas, F., Vazquez, T., & Grutzeck, M. (1999). Chemical stability of cementitious materials based on metakaolin. Cement and Concrete Research, 29(7), 997-1004.

Palomo, Á., Fernández-Jiménez, A., López-Hombrados, C., & Lleyda, J. L. (2011). Railway sleepers made of alkali activated fly ash concrete. *Revista Ingeniería de Construcción*, 22(2), 75-80

Petermann, J. C., Saeed, A., & Hammons, M. I. (2010). Alkali-activated geopolymers: a literature review. Air Force Research Laboratory, 1-92.

Phoo-ngernkham, T., Sata, V., Hanjitsuwan, S., Ridtirud, C., Hatanaka, S., & Chindaprasirt, P. (2015). High calcium fly ash geopolymer mortar containing Portland cement for use as repair material. *Construction and Building Materials*, 98, 482-488.

Puertas, F., Gutierrez, R. D., Fernández-Jiménez, A., Delvasto, S., & Maldonado, J. (2002). Alkaline cement mortars. Chemical resistance to sulfate and seawater attack. Materiales de Construccion, 52(267), 55-71.

Provis, J., Duxson, P., Van Deventer, J., & Lukey, G. (2005). The role of mathematical modelling and gel chemistry in advancing geopolymer technology. *Chemical Engineering Research and Design*, 83(7), 853-860.

Ramezanianpour, A. A. (2014). *Cement replacement materials*. Geochemistry/ Mineralogy. Springer.

Rangan, B. V. (2014). Geopolymer concrete for environmental protection. *The Indian Concrete Journal*, 88(4), 41-59.

Rashad, A., Bai, Y., Basheer, P., Milestone, N., & Collier, N. (2013). Hydration and properties of sodium sulfate activated slag. Cement and Concrete Composites, 37, 20-29.

Rashad, A. M. (2013a). A comprehensive overview about the influence of different additives on the properties of alkali-activated slag–a guide for civil engineer. *Construction and building materials*, 47, 29-55.

Rashad, A. M. (2013b). Properties of alkali-activated fly ash concrete blended with slag. *Iran Journal of Materials Science and Engineering, 10(1), 57-64.*

Rehan, R., & Nehdi, M. (2005). Carbon dioxide emissions and climate change: policy implications for the cement industry. *Environmental Science & Policy*, 8(2), 105-114.

Rodríguez, E., Bernal, S., De Gutiérrez, R. M., & Puertas, F. (2008). Alternative concrete based on alkali-activated slag. Materiales de Construcción, 58(291), 53-67.

Rostami A. (2015). Effective parameters on permeability of alkali-activated concretes". In: https: // www. civilica. com/ Paper-ICSAU03-ICSAU03_ 0052. html.

Rowles, M. & O'connor, B. (2003). Chemical optimisation of the compressive strength of aluminosilicate geopolymers synthesised by sodium silicate activation of metakaolinite. *Journal of Materials Chemistry*, 13(5), 1161-1165.

Puligilla, S. & Mondal, P. (2013) Role of slag in microstructural development and hardening of fly ash-slag geopolymer, *Cement and Concrete Research*, 43(1), . 70–80.

Salami, B. A., Megat Johari, M. A., Ahmad, Z. A. & Maslehuddin, M. (2016) „IN/mm2ct of added water and superplasticizer on early compressive strength of selected mixtures of palm oil fuel ash-based engineered geopolymer composites", *Construction and Building Material.* 109, 198–206.

Salau, M. A., & Olonade, K. A. (2011). Pozzolanic potentials of cassava peel ash. *Journal of Engineering Research*, 16(1), 10-21.

Salih, M. A., Abang Ali, A. A. & Farzadnia, N. (2014). Characterization of mechanical and microstructural properties of palm oil fuel ash geopolymer cement paste, *Construction and Building Materials*, 65, 592–603.

Salih, M. A., Farzadnia, N., Abang Ali, A. A. & Demirboga, R. (2015). Development of high strength alkali activated binder using palm oil fuel ash and GGBS at ambient temperature, *Construction and Building Materials*, 93, 289–300.

Santhanam, M., Cohen, M. D., & Olek, J. (2002). Mechanism of sulfate attack: A fresh look: Part 1: Summary of experimental results. Cement and concrete research, 32(6), 915-921.

Shetty, M. S. (2009). *Concrete technology: Theory and practice*. S. Chand & Company Ltd. New Delhi, India.

Singh, B., Rahman, M. R., Paswan, R. & Bhattacharyya, S. K. (2016). Effect of activator concentration on the strength, ITZ and drying shrinkage of fly ash/slag geopolymer concrete, *Construction and Building Materials*, 118, 171–179.

Soutsos, M., Boyle, A. P., Vinai, R., Hadjierakleous, A. & Barnett, S. J. (2016). Factors influencing the compressive strength of fly ash based geopolymers, *Construction and Building Materials*, 110, 355–368.

Söylev, T. A. & Özturan, T. (2014). Durability, physical and mechanical properties of fiber-reinforced concretes at low-volume fraction. *Construction and Building materials*, 73, 67-75.

Stern, N. H. (2007). The economics of climate change: the Stern review: cambridge University press.

Suksiripattanapong, C., Horpibulsuk, S., Chanprasert, P., Sukmak, P., & Arulrajah, A. (2015). Compressive strength development in fly ash geopolymer masonry units manufactured from water treatment sludge. *Construction and Building Materials*, 82, 20-30.

Temuujin, J., van Riessen, A., & MacKenzie, K. (2010b). Preparation and characterisation of fly ash based geopolymer mortars. *Construction and Building Materials*, 24(10), 1906-1910.

Thokchom, S., Ghosh, P., & Ghosh, S. (2009). Effect of water absorption, porosity and sorptivity on durability of geopolymer mortars. *ARPN Journal of engineering and Applied Sciences*, 4(7), 28-32.

Wang, W. C., Wang, H. Y. & Lo, M. H. (2015). The fresh and engineering properties of alkali activated slag as a function of fly ash replacement and alkali concentration, *Construction and Building Materials*, 84, 224–229.

Williamson, T. & Juenger, M. C. G. (2016). The role of activating solution concentration on alkali-silica reaction in alkali-activated fly ash concrete, *Cement and Concrete Research*., 83, 124 130.

Wilson, J. W., & Ding, Y. C. (2007). A comprehensive report on pozzolanic admixtures, the cement industry, market and economic trends and major companies operating in the Far East, with reference to Pagan Island. A Report Prepared for the Secretary, Department of Public Lands, Commonwealth of Northern Mariana Islands, 4-33.

Xie, J. & Kayali, O. (2014). Effect of initial water content and curing moisture conditions on the development of fly ash-based geopolymers in heat and ambient temperature", *Construction and Building Materials*, 67, 20–28.

Yao, X., Zhang, Z., Zhu, H., & Chen, Y. (2009). Geopolymerization process of alkali–metakaolinite characterized by isothermal calorimetry. *Thermochimica Acta*, 493(1), 49-54.

Yip, C. K., Lukey, G., &Van Deventer, J. (2005). The coexistence of geopolymeric gel and calcium silicate hydrate at the early stage of alkaline activation. *Cement and Concrete Research*, 35(9), 1688-1697.

Yong, M., Liu, J., Alengaram, U. J., Santhanam, M., Zamin, M. & Hung, K. (2016) Microstructural investigations of palm oil fuel ash and fly ash based binders in lightweight aggregate foamed geopolymer concrete, *Construction and Building Materials*, 120, 112–122.

Yusuf, M. O., Megat Johari, M. A., Ahmad, Z. A. & Maslehuddin, M. (2014) „Strength and microstructure of alkali-activated binary blended binder containing palm oil fuel ash and ground blast-furnace slag", *Construction and Building Materials*, 52, . 504–510.

Zhang, Z., Provis, J. L., Reid, A. & Wang, H. (2014). Geopolymer foam concrete: An emerging material for sustainable construction", *Construction and Building Materials*, 56, 113–127.

Zhang, Z., Yao, X., & Wang, H. (2012). Potential application of geopolymers as protection coatings for marine concrete III. Field experiment. *Applied Clay Science*, 67, 57-60.

Zhang, Z., Yao, X., & Zhu, H. (2010a). Potential application of geopolymers as protection coatings for marine concrete: II. Microstructure and anticorrosion mechanism. *Applied clay science*, 49(1), 7-12.

Zhang, Y., Cao, S.-X., Shao, S., Chen, Y., Liu, S.-L., & Zhang, S.-S. (2011). Aspen Plus-based simulation of a cement calciner and optimization analysis of air pollutants emission. *Clean Technologies and Environmental Policy*, 13(3), 459-468.

Zhang, Y. J., Wang, Y. C., & Li, S. (2010b). Mechanical performance and hydration mechanism of geopolymer composite reinforced by resin. *Materials Science and Engineering: A*, 527(24), 6574-6580.

Zhou, W., Yan, C., Duan, P., Liu, Y., Zhang, Z., Qiu, X. & Li, D. (2016). A comparative study of high- and low-Al_2O_3 fly ash based-geopolymers: The role of mix proportion factors and curing temperature, *Materials and Design.* 95, 63–74.

APPENDIX A: RESULTS OF THE EXPERIMENTAL WORK

Table A1: Mass loss of ternary blended GPMs subjected to Na_2SO_4 attack

Specimen Number	% mass loss (28 days)	% mass loss (56 days)	% mass loss (90 days)
PCM	29.60	32.20	32.40
C90M7R3	28.90	31.70	32.10
C70M20R10	22.40	23.60	25.59
C50M33R17	14.2	16.70	17.30
C30M47R23	19.1	22.30	21.90
C10M60R30	29.0	30.30	33.30

Table A2: Mass loss of ternary blended GPMs subjected to H_2SO_4 attack

Specimen Number	% mass loss (28 days)	% mass loss (56 days)	% mass loss (90 days)
PCM	31.25	33.30	34.10
C90M7R3	29.50	32.55	32.95
C70M20R10	24.20	23.99	26.45
C50M33R17	16.50	18.25	19.22
C30M47R23	20.25	25.05	26.59
C10M60R30	29.50	30.69	33.45

Table A3: Strength losses as caused by Na_2SO_4 attack on ternary blended GPMs (28 days)

Specimen	Curing Media		Strength Loss (N/mm^2)	Strength Loss Factor % (SLF)	Residual Strength (%)
	Ambient (N/mm^2)	Na_2SO_4 (N/mm^2)			
PCM	22.65	15.82	6.83	30.15	69.85
C90M7R3	24.56	18.05	6.51	26.51	73.49
C70M20R10	25.35	22.10	3.25	12.82	87.18
C50M33R17	39.25	38.58	0.67	1.71	98.29
C30M47R23	27.10	24.16	2.94	10.85	89.15
C10M60R30	26.85	22.80	4.05	15.08	84.92

Table A4: Strength losses as caused by Na_2SO_4 attack on ternary blended GPMs (56 days)

Specimen	Curing Media		Strength Loss (N/mm^2)	Strength Loss Factor % (SLF)	Residual Strength (%)
	Ambient (N/mm^2)	Na_2SO_4 (N/mm^2)			
PCM	25.23	15.92	9.31	32.89	67.02
C90M7R3	26.35	19.05	7.30	27.70	72.30
C70M20R10	30.05	25.86	4.19	13.94	86.06
C50M33R17	42.25	40.05	2.20	5.21	94.79
C30M47R23	33.26	29.10	4.16	12.51	87.49
C10M60R30	30.86	25.78	5.08	16.46	83.54

Table A5: Strength losses as caused by Na_2SO_4 attack on ternary blended GPMs (90 days)

Specimen	Curing Media		Strength Loss (N/mm^2)	Strength Loss Factor % (SLF)	Residual Strength (%)
	Ambient (N/mm^2)	Na_2SO_4 (N/mm^2)			
PCM	26.45	16.26	10.19	38.53	61.47
C90M7R3	28.86	20.70	8.16	28.27	71.73
C70M20R10	35.26	30.10	5.16	14.63	85.37
C50M33R17	44.65	39.98	4.67	10.46	89.54
C30M47R23	36.48	31.08	5.40	14.80	85.20
C10M60R30	32.96	25.86	7.10	21.54	78.46

Table A6: Strength losses as caused by H_2SO_4 attack on ternary blended GPMs (28 days)

Specimen	Curing Media		Strength Loss (N/mm^2)	Strength Loss Factor % (SLF)	Residual Strength (%)
	Ambient (N/mm^2)	Na_2SO_4 (N/mm^2)			
PCM	26.45	18.05	8.51	32	68
C90M7R3	28.26	19.75	8.40	30	70
C70M20R10	29.56	24.31	5.25	18	82
C50M33R17	41.36	38.69	2.67	6	94
C30M47R23	30.16	25.22	4.94	16	84
C10M60R30	29.86	23.81	6.05	20	80

Table A7: Strength losses as caused by H_2SO_4 attack on ternary blended GPMs (56 days)

Specimen	Curing Media		Strength Loss (N/mm^2)	Strength Loss Factor % (SLF)	Residual Strength (%)
	Ambient (N/mm^2)	H_2SO_4 (N/mm^2)			
PCM	29.20	17.89	11.31	39	61
C90M7R3	30.26	20.96	9.30	32	68
C70M20R10	32.68	26.49	6.19	19	81
C50M33R17	43.65	39.45	4.20	10	90
C30M47R23	34.20	28.04	6.16	18	82
C10M60R30	31.45	24.37	7.08	23	77

Table A8: Strength losses as caused by H_2SO_4 attack on ternary blended GPMs (56 days)

Specimen	Curing Media		Strength Loss (N/mm^2)	Strength Loss Factor % (SLF)	Residual Strength (%)
	Ambient (N/mm^2)	H_2SO_4 (N/mm^2)			
PCM	28.86	16.67	12.19	42	58
C90M7R3	30.25	20.09	10.16	34	66
C70M20R10	36.88	29.72	7.16	19	81
C50M33R17	45.36	38.69	6.67	15	85
C30M47R23	38.35	30.95	7.40	19	81
C10M60R30	34.56	25.46	9.10	26	74

Table A9: Water Absorption of ternary blended GPMs

Specimen number	28 days (%)	56 days (%)	90 days (%)
PCM	16.34	16.65	16.89
C90M7R3	16.07	16.25	16.35
C70M20R10	15.46	15.65	15.95
C50M33R17	10.0	10.12	10.25
C30M47R23	13.78	13.89	14.01
C10M60R30	15.92	16.05	16.14